Structural Engineering Report No. 114

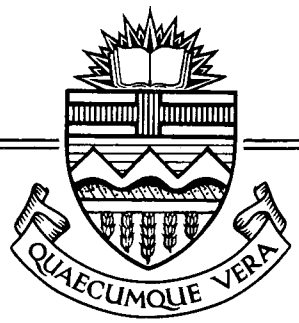

EXPERIMENTAL STUDY OF STEEL PLATE SHEAR WALLS

by
P. A. TIMLER
and
G. L. KULAK

November, 1983

EXPERIMENTAL STUDY OF STEEL PLATE SHEAR WALLS

by

P.A. Timler

and

G.L. Kulak

DEPARTMENT OF CIVIL ENGINEERING

THE UNIVERSITY OF ALBERTA

EDMONTON, ALBERTA

November, 1983

Abstract

The use of steel plate shear walls to resist lateral forces in multi-storey structures is a new and innovative design technique. Although a significant number of buildings have been constructed using the method, design has tended to be conservative, reflecting the lack of physical testing of the system. The basis of current design methods is that shear buckling of the panel be precluded in order that the shear yield stress level be reached. The result is that either the panels are relatively thick, or that frequent stiffeners are required.

A study which reviewed existing steel shear wall systems and developed a new analytical approach for their design was reported in 1982 by Thorburn, Kulak, and Montgomery (1). Their proposal considers that the resistance of the steel panel consists of post-buckling strength alone, attained by the development of a tension field within the plate. The model treats the tension field as a series of inclined bars, each acting under uniaxial tension. The method identifies the post-buckling strength in a similar, but not identical, way to that used in plate girder design.

In order to substantiate the proposed analytical method of Thorburn, et al., it was necessary to undertake physical testing of the system. The results and evaluation of that testing program are the subject of this report. A large scale, single storey specimen was tested under;

1) a cyclic loading to the serviceability limit,

2) loading to failure,

in order to examine the adequacy of the proposed post-buckling model. The framing scheme used reasonably-sized structural components and was fabricated in accordance with normal shop procedures. Good agreement was obtained between the actual and predicted stresses in the various components and in the load-deflection response of the frame. This good agreement implies that the proposed design approach is satisfactory. Of equal importance was the evaluation of system performance under working loads. The test showed that the buckles which formed in the web under application of a load equal to that corresponding to the storey drift limit, disappeared entirely when the load was removed. Valuable information was also obtained on the performance of connection details.

Acknowledgements

This report is based on the thesis submitted by Peter Adam Timler to the Faculty of Graduate Studies and Research at the University of Alberta in partial fulfillment of the requirements for the degree of Master of Science in Civil Engineering. During the period of his studies, he received financial support from the Alberta Regional Committee of the Canadian Institute of Steel Construction and from the Province of Alberta.

The project was sponsored by the American Iron and Steel Institute and was directed by an advisory committee consisting of J.W. Hotchkies, E.Y.L. Chien, R.M. Richard, and A.C. Kuentz.

The authors are grateful for the financial assistance received and acknowledge with thanks the helpful comments and direction provided by the advisory committee.

Table of Contents

Chapter Page

1. Introduction 1

1.1 Statement of Problem 1

1.2 Objectives 4

2. Literature Survey 5

2.1 Origins of Tension Field Theory 5

2.2 Diagonal Tension in Plate Girders 6

2.3 Proposed Steel Plate Shear Wall Design 7

2.4 Current Design Approaches 8

2.5 Previous Testing 12

3. Experimental Program 16

3.1 Scope 16

3.2 Coupons 17

3.3 Full Scale Test Specimen 17

3.3.1 Description 17

3.3.2 Test Set-Up 19

3.3.3 Test Procedure 20

3.3.4 Data Acquisition 21

4. Test Results 28

4.1 Introduction 28

4.2 Coupon Tests 28

4.3 Full Scale Test to Service Loads 28

4.3.1 Web Plate Stresses 28

4.3.2 Strains in Framing Members 31

4.3.3 Frame Deflection 33

4.3.4 Web Plate Deflection 33

4.4 Full Scale Test to Ultimate Load 35

4.4.1 Definition of Limits 35

4.4.2 Web Plate Stresses 35

4.4.3 Strains in Framing Members 37

4.4.4 Frame Deflection 38

4.4.5 Web Plate Deflection 38

5. Comparison of Analytical and Experimental Results ...65

5.1 Introduction 65

5.2 Web Plate Stresses at Predicted First Yield 65

5.3 Strains to Failure in Framing Members 66

5.4 Frame Deflection to Failure 67

5.5 Factors Affecting Failure 71

5.6 Sources of Errors 72

5.6.1 Instrumentation Errors 72

5.6.2 Geometrical Differences 73

6. Summary, Conclusions and Recommendations 81

6.1 Summary and Conclusions 81

6.2 Recommendations 83

6.2.1 Fabrication Techniques 83

6.2.2 Future Testing 84

References 85

Appendix A - Formula Derivation for Angle of Inclination of Tension Field 88

A.1 Formula Derivation 89

Appendix B - Determination of Angle of Inclination of Tension Field for the Test Specimen 99

B.1 Theoretical Value of Tension Field Angle 100

List of Tables

Table		Page
4.1	Full Scale Specimen Test History	40
4.2	Coupon Test Results	41
4.3	Web Deflection Summary at Service Loads	41

List of Figures

Figure		Page
2.1	Plane Frame Model	15
3.1	Full Scale Specimen	24
3.2	Overall Test Set-Up	25
3.3	Lower Pin Arrangement	25
3.4	Gauge Locations and In-Plane Deflection Instrumentation	26
3.5	Orientation of Web Deflection Measurement Device	27
3.6	Close-Up of Web Deflection Transducer and Track	27
4.1	Unaveraged Principal Stress Readings, Test #3	42
4.2	Averaged Principal Stresses, 1st Comp. Cycle, Test #3	43
4.3	Averaged Principal Stresses, 1st Tens. Cycle, Test #3	44
4.4	Averaged Principal Stresses, 2nd Comp. Cycle, Test #3	45
4.5	Averaged Principal Stresses, 2nd Tens. Cycle, Test #3	46
4.6	Section 2 - Axial and Bending Strains, Test #3	47
4.7	Section 4 - Axial and Bending Strains, Test #3	48
4.8	Section 5 - Axial and Bending Strains, Test #3	49
4.9	Section 4 - Absolute Strains, Tests #2 and #3	50
4.10	Load vs Deflection, Tests #2 and #3	51
4.11	Web Deflection, Test #1	52
4.12	Web Deflection, Test #2	53
4.13	Web Deflection, Test #3	54

Figure Page

4.14 Averaged Principal Stresses, First Yield, Test #4.....55

4.15 Averaged Principal Stresses, Ultimate Load, Test #4 - #5.....56

4.16 Section 1 - Absolute Strains, Test #4 - #5.....57

4.17 Section 2 - Absolute Strains, Test #4 - #5.....58

4.18 Section 3 - Absolute Strains, Test #4 - #5.....59

4.19 Section 4 - Absolute Strains, Test #4 - #5.....60

4.20 Section 5 - Absolute Strains, Test #4 - #5.....61

4.21 Load vs Deflection, Test #4 - #5.....62

4.22 Weld Tear of Fish Plate Connection at 5200 kN.....63

4.23 Web Deflection, Test #4.....64

5.1 Predicted vs Experimental Web Stresses at Yield.....75

5.2 Section 2 - Predicted vs Experimental Strains.....76

5.3 Section 4 - Predicted vs Experimental Strains.....77

5.4 Section 5 - Predicted vs Experimental Strains.....78

5.5 Predicted vs Experimental Frame Deflection.....79

5.6 Predicted Frame Deflection Curves.....80

A.1 Shear Core Subjected to Lateral Load.....90

A.2 Balancing Tension Fields.....91

A.3 Free-Body Diagram of Portion of the Web.....92

A.4 Column Free-Body Diagram.....93

A.5 Strip Model Representation.....95

List of Symbols

A.....General cross-sectional area

A_b.....Beam area

A_c.....Column area

A_w.....Web plate area

E.....Modulus of elasticity

h.....Shear panel height

I.....General cross-sectional moment of inertia

I_b.....Beam moment of inertia

I_c.....Column moment of inertia

L.....Shear panel length

M.....General member moment

M_c.....Column moment

P.....General member axial force

R.....Total web plate force

R'.....Portion of web plate force

V.....Applied shearing force

W.....General work done

W_b.....Beam work done

$W_{c_{Axial}}$.....Column axial work done

$W_{c_{Bend}}$.....Column bending work done

W_{Total}.....Total work done as a result of the tension field

W_w.....Web work done

α.....Angle of inclination of the tension field

σ.....General stress

σ_w.....Web plate stress

1. Introduction

1.1 Statement of Problem

Of the many schemes used for resisting lateral load in the design of high rise structures, one of the newest and most innovative is the steel plate shear wall core. Shear walls have proven to be an effective bracing system for buildings in the fifteen to forty storey range where they usually surround the interior service area of the structure. Lateral forces applied on the exterior walls of the building are transmitted to the core by means of diaphragm action. Until recently, shear cores have been constructed almost exclusively of reinforced concrete, regardless of whether the main structural frame was concrete or steel.

The design approach that has been used for steel shear walls has been to provide the lateral restraint required through the shear resistance of the web plate located in the core. This shear resistance is calculated on the basis either of attainment of shear yield in the plate or the stress that will produce shear buckling of the plate. Any additional strength that may be present after the web has buckled is neglected.

A number of buildings have been constructed using steel plate shear walls, most notably in the United States and Japan (1). Although the design basis appears to be the same in each area, fabrication practice differs. In Japan designers have extensively employed longitudinal and transverse

stiffeners of various cross-sectional shapes on both sides of the steel plate. This ensures that the yield stress limit of the web material would be reached prior to any lateral buckling of the plate. The approach favoured by the American designers consists of fewer (or no) stiffeners; however this requires a thicker web plate in order to meet the buckling stress limitation. In both instances, the web plate is, of course, enclosed by a beam and column framework to complete the shear wall panel. While both of these design techniques have proven in many cases to be competitive with moment resisting frames and concrete shear cores, the strength provisions are apparently conservative.

Since Basler's work on plate girders published in 1961 (2), it has generally been acknowledged in civil engineering practice that a thin web can have considerable post-buckling strength. The additional strength exists as a result of the development of a tension field within the web plate as it deforms. The magnitude of the post-buckling strength is largely dependent on the effective anchoring of the tension field. This, in turn, is a function of the bounding elements of the panel, which are the flanges and transverse stiffeners in the case of a plate girder. The largest contribution of this secondary strength effect occurs when the perimeter of the web exhibits infinitely stiff characteristics.

An obvious analogy exists between the plate girder and a shear wall core subjected to a lateral load. Realizing that a steel plate shear wall core, framed by columns and

girders is essentially the same as the web of a plate girder panel bounded by flanges and transverse stiffeners, it has been proposed (1) that the post-buckling resistance be utilized in calculating the strength provided by a steel plate core.

Like plate girder webs, the out-of-flatness of a steel plate in a shear core is unlikely to constitute a strength limit since the web is, inevitably, initially out-of-flat. This is expected to arise from the fabrication and handling of steel shear wall tiers when relatively thin plates are used. Therefore a buckled condition may be assumed to exist prior to loading and any loading applied to the frame can only be carried as the result of the immediate development of a tension field. However, if the web buckles or is initially buckled under service loads, it is imperative to know the magnitude of deformation in order to evaluate its effects on the bonding between the web plate and fireproofing materials. Consideration must also be given to the clearance tolerances between mechanical or electrical services located within the core and the shear wall. Furthermore, the behavior of the buckled plate when subjected to load reversals is unknown.

The analytical approach recently presented by Thorburn, et al. (1) is an attempt to account for this post-buckling strength. Following upon this work, an experimental program was undertaken to verify that unstiffened, thin-webbed steel plates are effective as a lateral load resisting scheme.

1.2 Objectives

The objectives of this investigation are:

1) To observe the actual tension field present within a large scale shear wall test specimen subjected to shear.
2) To compare actual test data with results obtained from the proposed analytical method.
3) To recommend additional design considerations and fabrication techniques.
4) To indicate areas of interest for future investigation.

2. Literature Survey

2.1 Origins of Tension Field Theory

Wagner was the first to recognize that the load-carrying capacity of thin-webbed structural members was not limited to the load which corresponded to web buckling (3). From his experimental investigation of flat sheet metal girders subjected to shear, he demonstrated that a diagonal tension field forms during buckling. Upon attainment of buckling, the load-carrying mechanism performs much like a Pratt truss wherein the inclined folds behave as a series of tension diagonals anchored to the stiffeners. By showing that loads many times greater than those which produce buckling could still be carried by the web-stiffener arrangement, the traditional structural design approach then used in the aviation industry was improved.

Because the webs used in aeronautical design are so thin, the force required to produce the theoretical web buckling load is relatively small; it is customary to ignore this contribution when calculating the total capacity. Furthermore, since the surrounding framing members are much stiffer than the web itself, a complete tension field develops throughout. Wagner proposed a unique strip model representation encompassing both of these concepts for the strength prediction of thin-webbed aircraft membrane.

Following Wagner's study, designers considered the ultimate strength of a shear web as being in either of two

categories. Webs could be deemed as "shear resistant", wherein instability was not permitted prior to yield, or as "pure diagonal tension webs", in which case the shear carried by the web before buckling was disregarded. Kuhn et al. (4), elaborated on the theory brought forth by Wagner by introducing the idea of incomplete diagonal tension and proposed a method of interpolating between the two extremes postulated by Wagner. The proposed solution involved a trial and error procedure if the flanges bounding the shear panel were not infinitely stiff, thus limiting its application.

2.2 Diagonal Tension in Plate Girders

Basler applied the developments of Wagner and Kuhn, made with particular reference to the aircraft industry, to civil engineering structures (2). He judged that, because of the relatively low bending strength in the flanges of a plate girder, the tension field would develop only partially. Basler also considered the ultimate strength of the web-plate girder as the contributions of two parts; the shear capacity of the web due to beam action and the additional resistance of the web from the formation of the tension diagonals following buckling.

Although many variations of tension field theory have since been introduced for plate girders (5,6), their differences lie largely in the configuration of the assumed tension band and the type of failure mechanism used to define it. Most provide solutions which are marginally better than

Basler's but since they tend to be more complicated, Basler's approach is still favoured. This is reflected through its incorporation in the major North American steel codes.

2.3 Proposed Steel Plate Shear Wall Design

As previously noted, a steel plate shear wall core, consisting of relatively thin steel plates bounded by columns and beams, bears an obvious resemblance to a conventional plate girder. The columns in the shear wall core play the same role as the plate girder flanges, the beams or girders in the frame act as stiffeners, and the steel plate behaves as the web. Thorburn, et al. (1), developed an analytical procedure for this case. Recognizing that the columns are relatively stiff as compared to the flanges of a plate girder, they used the original approach developed by Wagner and Kuhn rather than that proposed by Basler. On the assumption that the steel plate shear wall webs are either already buckled upon completion of fabrication or are so thin as to buckle under low loads, only post-buckling strength was considered.

The angle of inclination of the tension field, α, was developed by Thorburn, et al. on the basis of least energy absorbed by the panel when subjected to shear. It has been recognized subsequently that the potential energy development used did not include the bending effects in the columns. This discrepancy is examined in Appendix A of this

report.

A strip model representation of inclined tension members, again similar to that of Wagner, was introduced by Thorburn, et al. The model, shown in Figure 2.1, uses a series of tension struts oriented at an angle α to represent the web. They are assumed to be pin-connected to the adjoining framing members. A plane frame program based on the stiffness approach is used to analyze this model. Furthermore, a time-saving design technique of replacing the tension zone of the steel plate with an equivalent truss element having the same storey stiffness was suggested for the design stage of a multi-lift stack of shear wall elements. The size of the equivalent truss member was shown to be dependent upon the extent of tension field formation and its angle of inclination. This was similar to reported Japanese approaches for calculating the bending stiffness of a reinforced steel plate, as will be discussed in the following section.

2.4 Current Design Approaches

It appears that structures using steel plate shear walls have been constructed only in Japan and the United States. There is evidence, however, that increasing interest is developing in other parts of the world, notably Australia and Canada.

Limitation of local buckling stresses during transfer of the lateral loads through the shear wall element has been

of premium importance to the Japanese designers. The web plates are assumed to carry no gravity load and are extensively stiffened both laterally and transversely to prevent shear buckling. In the analysis of the structure as a whole, the shear resistance of the plates has been idealized as a series of diagonal tension and compression braces, both able to perform simultaneously. By assuming the extension of a single diagonal brace to be equivalent to the shear deflection of an unbuckled web plate, the areas of the braces can be calculated. Sway effects of the structures can then be examined using analyses founded on the stiffness approach. The final designs were based on the resulting restrictions of the deflection tolerances and assurance that material behavior remained within the elastic range.

Similarily, the method used by the American engineers in the design of steel shear wall buildings also restricts the out-of-plane buckling of the plates. It is implied (7,8) that proportioning of the steel plate ensures that the stresses are maintained below the critical buckling stress under service load conditions. This is achieved through the use of the same stiffened plate concepts as practiced in naval architecture for the design of steel bulkheads. Although a finite element analysis was used to check the results of the hand calculations, excellent agreement between the two approaches verified that the simplistic manual method was satisfactory for design purposes.

A recent publication (9), presents a design example for a typical shear panel in the Veterans Administration Medical Center in Charleston, South Carolina. The method offered was intended for steel shear wall design in existing buildings in order to provide a stiffer structure. A dynamic modal analysis was used to obtain the appropriate forces for the shear walls. A simple finite-element model was then used to calculate the membrane stresses. This analysis treated the steel shear panel as being independent of the concrete frame to which the steel plate was attached, an obviously conservative approach. Once the internal plate stresses were known, each panel was checked for either of the following conditions; plate buckling for shear only, or, plate buckling due to both in-plane shear forces and bi-axial compressive forces. The plate thickness was adjusted accordingly to meet the stress limitations. Both the vertical and horizontal stiffeners between the panels were designed as columns, similar to the way in which a bearing stiffener is designed.

At least one major difference exists between the Japanese and American hypotheses on load transfer through the structure. The latter examines some shear walls as gravity load bearing walls, that is, at least a portion of the vertical loads are transferred by the plate. This accounts for the extra plate thickness exhibited in the webs of North American steel shear wall structures.

Recent work in Australia (10,11) has produced an analytical procedure that differs somewhat from the methods

used by either the American or Japanese designers. A twenty storey building was studied by Angelidis and Mansell (10) in order to examine the behavior of a steel shear core subjected to lateral forces.

Under a wind loading, the core was analysed as a planar wall in each orthogonal direction using simple flexural theory. Where web openings such as corridors existed, a manual analysis of the structural interaction using the method proposed by Coull and Choudhury (12) for shear walls was used. Consideration for the shear lag effect, composed of the shear deformations in the coupling beams and the local deformations at the beam-to-wall junction, was made by reducing the moment of inertia of the coupling beam by published recommended amounts (13,14). Since geometric orthotropy of the stiffened steel plate was modelled by material orthotropy, different elastic moduli in the two principal directions idealized the stiffeners as being smeared throughout the panel width.

Based on the compressive loads obtained from the analysis, an average thickness was determined for the stiffened plate. When deflection and shear limitations had been achieved with this smeared plate thickness, the appropriate stiffener arrangement and plate thickness was then chosen from a stock of sizes previously designed and based on performance criteria obtained from box-girder research. It is not known whether any structures have been designed using this method, nor does there appear to have been any physical

testing conducted.

2.5 Previous Testing

Although many tests related to tension field behavior have been carried out over the last fifty years, only one major experimental program has been performed with the specific intent of modelling a steel shear core for structural consideration. Investigators for a large Japanese contracting firm, conducted a two-phase testing program on thin steel shear walls subjected to alternating horizontal loads (15). Several steel shear wall structures in Japan were subsequently designed based on methods of analysis derived from the basic principles established in this research.

Because Japan is located in a region of high seismic activity, the structural response and ductility relative to horizontal load reversals was of prime interest to the researchers. The first phase of the program encompassed the testing of twelve individual panels with overall dimensions of 2100 mm by 900 mm. Combinations of different stiffener arrangements with the various web plate thicknesses (2.3 mm to 4.5 mm) provided no duplication of test specimens. Real column and beam sizes were chosen to frame the panels, and members were pin-connected at the joints. The framing members were further stiffened to approximate an infinitely stiff boundary surrounding the web plate. The conclusions drawn regarding the strength and stiffness characteristics of steel shear walls after several load reversals were

applied to each test panel were as follows;

1) Superior buckling stability is obtained by stiffening both sides of the web as opposed to reinforcing one side only.
2) The hysteresis loop exhibited by the framing scheme is not altered by varying the stiffener orientation.
3) Sufficient ductility was provided by all the plate and stiffener arrangements tested.

Phase two of the program focused on the testing of two full scale prototypes of single bay, double storey lifts representing the tiers of a 32 storey shear core building being designed concurrent with the testing program. The test models differed from one another in that only one had openings in the web. The stiffeners were designed for these specimens using the results obtained in the first series of tests. The design criterion ensured that the elastic limit of the web plate was achieved prior to plate instability. However, once this limit had been exceeded, only a local buckling of the web was allowed between the reinforcing. This implies that the overall framework of beams, columns and stiffeners had to remain in-plane. These conditions were met easily by utilizing plate stability concepts in the design of the strengthening ribs.

An elasto-plastic finite element method was used under two assumptions to verify the results of the second series of tests. The stipulations were that the entire steel wall

would never buckle and that the material exhibit a bi-linear stress-strain relationship under the von Mises' criterion of yielding. Because of good agreement between the test results and the predicted load deflection curves it was concluded that the stiffeners could be designed based on the findings of the first phase. Furthermore, shear theory, wherein the shear transfer mechanism is displayed by beam action alone, could be used to establish the strength and rigidity of the stiffened plates provided the stresses are maintained below the critical shear buckling stress.

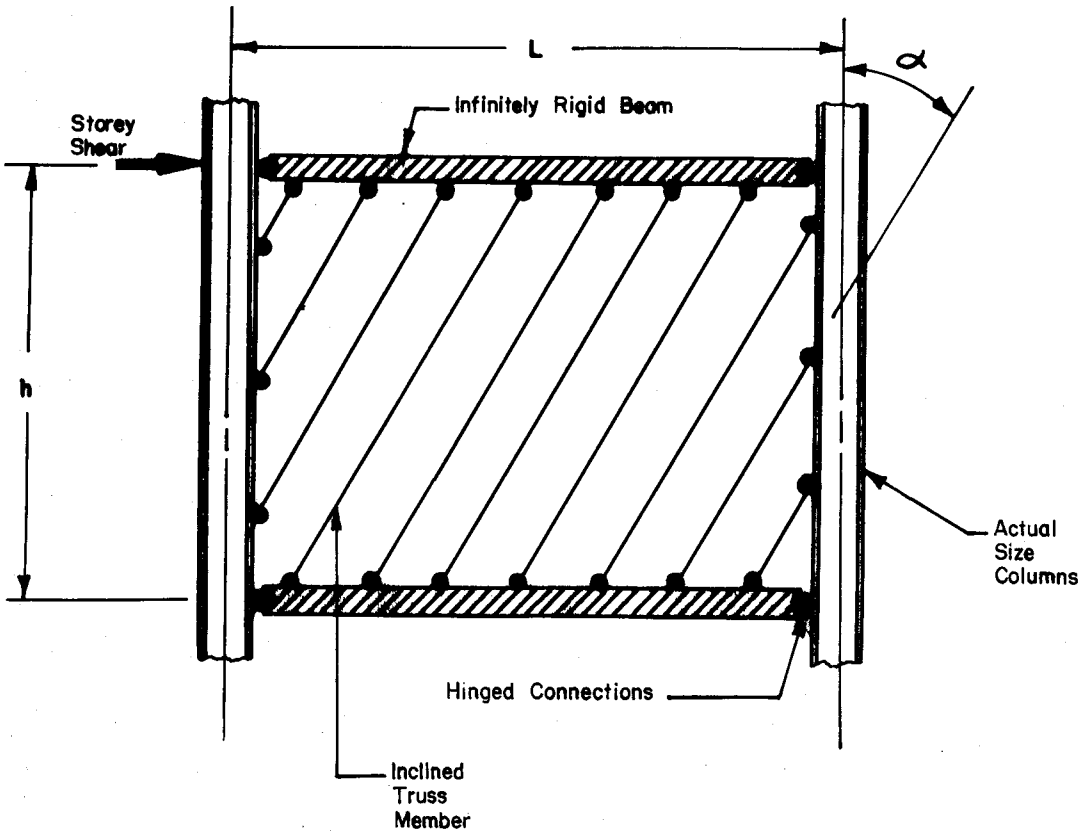

Figure 2.1 Plane Frame Model

3. Experimental Program

3.1 Scope

In order to substantiate the analytical proposal of Thorburn, et al. (1), a single full scale specimen was fabricated and tested. The major areas of interest of the testing program were the examination of the tension field development within the web plate and the deformation behavior of the plate under service load reversals.

Figure 3.1 shows the symmetric specimen tested. It represents two single storey, one bay steel shear wall elements. The members oriented vertically in the test specimen correspond to the beams in the prototype; the horizontal members in the test specimen represent the columns. The use of a symmetric model provided a condition of infinite stiffness at the interior beam located vertically at the center of the specimen. By having equal and opposing transverse (horizontal) components of the tensile forces present within both web plates acting on either side of the interior beam, a situation of no bending exists for this member. This is consistent with the usual design assumption for interior beams located in shear wall stacks (1).

The usual approach to modelling a framing network within a core considers beam-to-column connections as pin-jointed. This results from the fact that in actual construction practice, bolted web framing angles are most oftenly used to provide the connection detail. It was initially hoped that a

severe test of the practical pinned frame surrounding the steel panel could be made by utilizing true pin-connections at all the beam-to-column junctions. However, since the expected frame deflections from such a test specimen were relatively large (even at service load levels) with respect to practical testing limits, continuous connections were incorporated at the interior beam-to-column centerline junctions while true pin-connections were placed at the remaining (exterior) connections. This greatly reduced the panel deflection, thereby allowing for an uncomplicated test set-up.

3.2 Coupons

The web of the specimen was made from material supplied to CSA Specification G40.21 300W (16) (minimum specified yield strength of 300 MPa). In order to determine the actual static yield stress, a series of three coupon tests were performed on material cut from the same stock as subsequently used for the web panels.

3.3 Full Scale Test Specimen

3.3.1 Description

The full size test specimen, as shown in Figure 3.1, presented a dual test of two single shear wall panels each with dimensions corresponding to the centerlines of the framing members, that is, a bay width of 3750 mm and a storey height of 2500 mm. The columns, located horizontally,

were built-up sections approximately equivalent to a W310X129. The vertically oriented members, the beams in the prototype, were also built-up sections. They were approximately equivalent to W460X144 sections. These dimensions and framing sizes were chosen as representing reasonable structural proportions. Although the beam size chosen is probably somewhat larger than that expected in actual construction practice with respect to the column size, its cross-sectional properties were necessary in order that the tension field in the steel plate web have a satisfactory boundary.

Since the purpose of the experimental program was to test a thin-webbed steel shear wall, the thinnest hot-rolled plate readily available was obtained. A 5 mm web plate was selected. It was connected to the adjacent framing members by means of the fish plate arrangement depicted in Section A-A of Figure 3.1. The web plate was aligned such that its plane coincided with the planes of the webs of the beams and columns. The eccentricity introduced by the one-sided fish plate connection would have a subsequent effect on the final failure.

The beam-to-column connections at the centerline of the test specimen were continuous. Complete penetration groove welds were used and stiffeners were provided between the flanges of the interior beam in line with the flanges of the connecting columns.

The web regions surrounding the four pin-connections required doubler plates in order to provide sufficient

bearing area for the pin loads. The lower pins also functioned as reaction locations for both portions of the load cycle. The loading tongue located at the top of the central beam was designed to accommodate the service load reversals.

It was required that all steel except that used for the pins meet CSA Specification G40.21 300W. The pins were fabricated from steel with a minimum specified yield strength of 700 MPa.

3.3.2 Test Set-Up

The fabricated structure was tested as a simply supported deep beam. Because of the symmetry, two shear panels were thereby tested. This is shown in the overall test set-up of Figure 3.2. The loading was applied vertically at mid-span with reactions to the floor being transferred at the ends. A pin-connected clevis delivered the loads from the crosshead of the 6700 kN capacity MTS testing machine to the top of the interior beam.

A frame was erected which surrounded the specimen and provided the lateral bracing for the exterior (vertical) beams. Two articulating braces per beam were used, as seen in Figure 3.2, (one at the top, the other at the center of the beam) to restrict any out-of-plane movement. These braces also served to correct the slight twist that was present initially in the specimen, probably induced by the welding stresses from fabrication and by the transport procedure. Lateral restraint for the bottom of the exterior beams was

provided by wedging the specimen against the reaction tongues at the lower pin-connections as shown in Figure 3.3.

Although restraint would be provided by the testing machine specimen connection at the top of the central beam, a precautionary measure was taken by providing additional restraint using HSS sections as braces on either side of the web of the beam, shown in Figure 3.2. A further brace point was provided at the bottom of the interior beam.

A complete description of the strain and deflection measurement systems used is discussed in Section 3.3.4.

3.3.3 Test Procedure

Two loading sequences were used during the testing of the specimen; a cyclic loading to the allowable serviceability deflection limitation, and a final loading excursion until failure of the structural system was reached.

During the load reversals carried out within the first loading procedure, both tensile and compressive forces were applied. This was accommodated by the yoke and tongue arrangement previously mentioned in Section 3.3.2. The specimen was cycled three times such that the maximum permissible drift limit according to CSA S16.1 (h/400) was reached during each excursion (16). This corresponded to a deflection at the centerline of the test specimen of 6.25 mm, and it was attained by application of a 2104 kN load. Both strain and deflection readings (in-plane and out-of-plane) were being recorded at the end of each loading step.

Because the compressive loads expected to be attained during the second phase of testing were much greater than the capacity of the loading yoke, it was removed and replaced by the compression head of the testing machine following the completion of the load reversal excursions. The specimen was then gradually loaded in compression until the ultimate load of the framework was attained. Data were recorded at discrete intervals.

3.3.4 Data Acquisition

Four types of data acquisition were used during the entire testing program to fully describe any strain and deflection activity. These comprised rosette strain gauges, uni-axial strain gauges, dial gauges along with transducers, and, finally, out-of-plane deflection monitoring of the panel web.

Rosette strain gauges were mounted extensively, particularly on one of the two identical panels, in order that principal strains and their associated directions could be obtained within the web plate. Figure 3.4 shows the gauging locations as well as some of the in-plane deflection instrumentation. The circled gauges on the left panel indicate that rosettes were placed on the backside of the plate directly opposite those on the front side. This duplication of gauges was done in order to account for the bending stresses expected to occur within the plate as a result of buckling. A much smaller number of rosettes were placed on the other

panel, primarily for the use as a check on the assumed equal distribution of the strains throughout the symmetrical specimen. Four additional strain gauges, two on either side of the right hand panel, were added to the lower interior corner prior to the final testing of the specimen. They were placed there to examine better the yield band developing in an unbuckled region.

Uni-axial strain gauges were placed on various cross-sections of the beams and columns in order to monitor their loads. A comparison between the predicted load distribution and those achieved experimentally would eventually be obtained from these results. The five cross-sections with gauging locations shown are also indicated in Figure 3.4.

Dial gauges numbered 1 through 4 (Figure 3.4) were used to record the settlement and axial deformation of the exterior beams. During tension loading, the uplift of the base plates was also recorded. Additional dial gauges were placed perpendicular to the hold-down reaction points during higher load increments to observe any lateral movement of the reaction tongues. Similarily a dial gauge was placed at the center of the interior beam, transverse to the web, to monitor any lateral instability. Transducers were placed at the top and bottom of the central column to record the axial deformation and absolute deflection of the frame. The stroke as obtained from the ram of the testing machine was also monitored as a check.

A web deflection measurement device was constructed to maintain a continuous record of the profile of the buckled web plate perpendicular to the inclination of the folds formed. This device, shown in Figures 3.5 and 3.6, consisted of a modified transducer mounted on a buggy which ran along a rail system. The tip of the transducer was equipped with a ball bearing to eliminate any friction when travelling along the surface of the plate. The transducer was located at right angles to the web, and constant contact with the plate surface was provided by a coil spring located on its shaft. The buggy to which the transducer was attached traversed the rail through power supplied to a motor and cable arrangement. Continuous recording of the position of the buggy along the track was obtained through voltage readings received from a potentiometer connected to the cable system. Simultaneously, immediate data was recorded on an X-Y plotter during testing as well as being stored on a mini-computer.

Prior to testing, most of the specimen was whitewashed to aid in the visual identification of yielding regions.

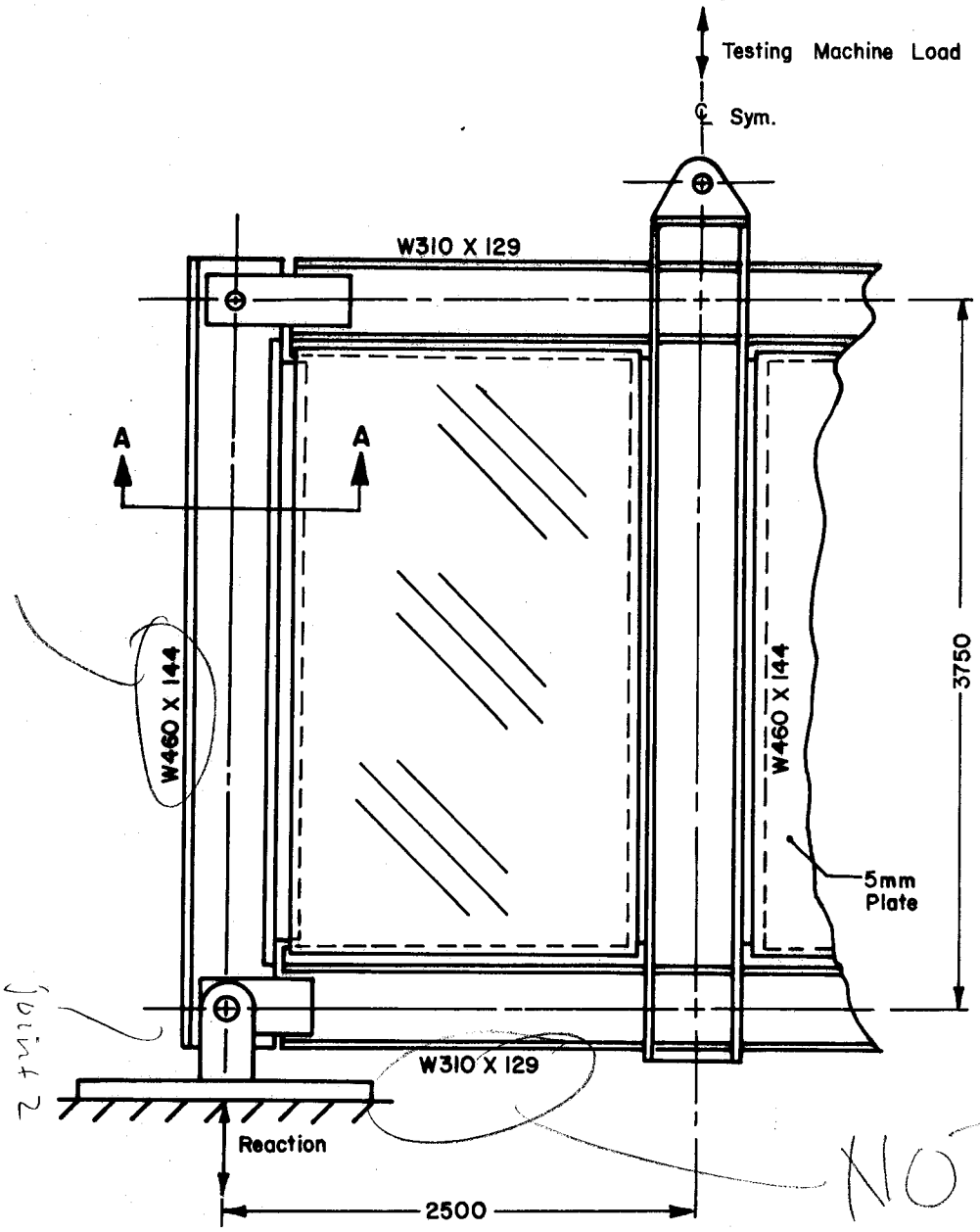

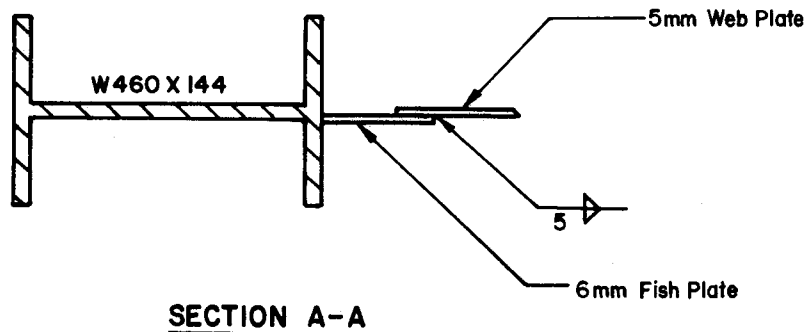

SECTION A-A

Figure 3.1 Full Scale Specimen

W460 x 144, from CISC
A = 18400
I_x = 726 x 10^6
P.T's values (Appendix B)
A = 20952
I_x = 810.3 x 10^6

W310 x 129, from CISC
A = 16500
I_x = 308 x 10^6
P.T's values (Appendix B)
A = 15656
I = 295.4 x 10^6

P.T's values calculated from dimensions given in shop drawings, not measured ones.

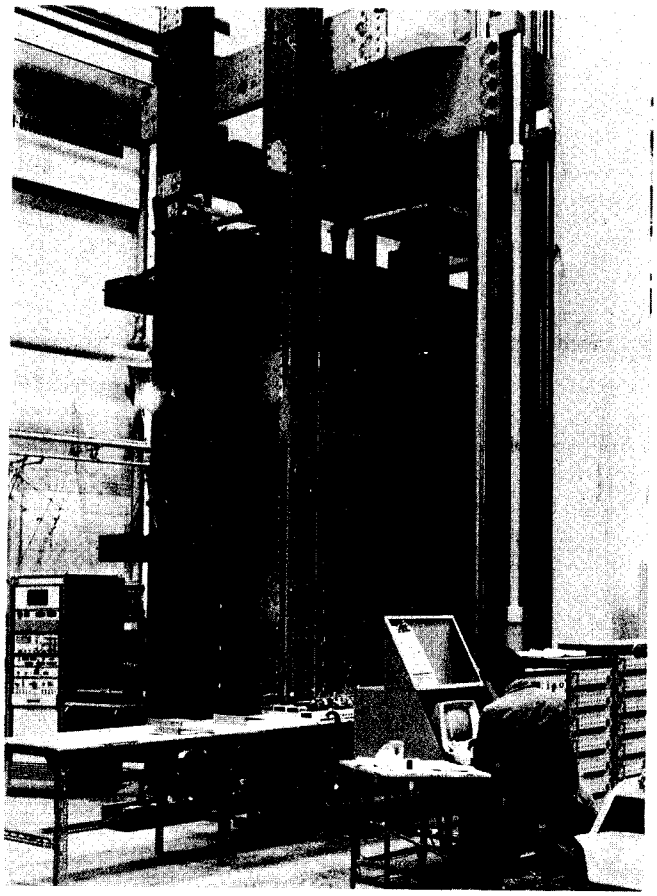

Figure 3.2 Overall Test Set-Up

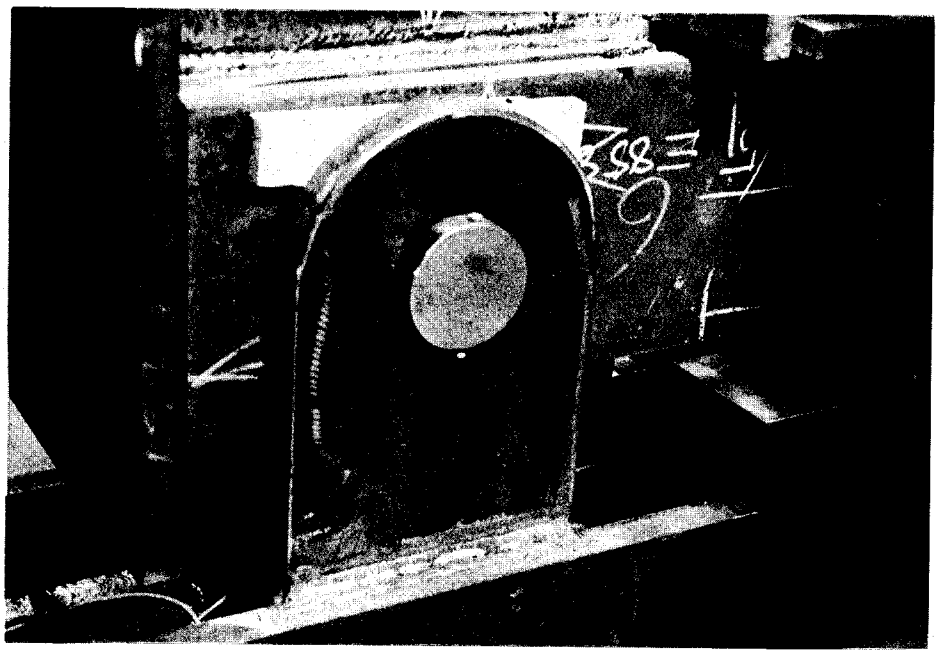

Figure 3.3 Lower Pin Arrangement

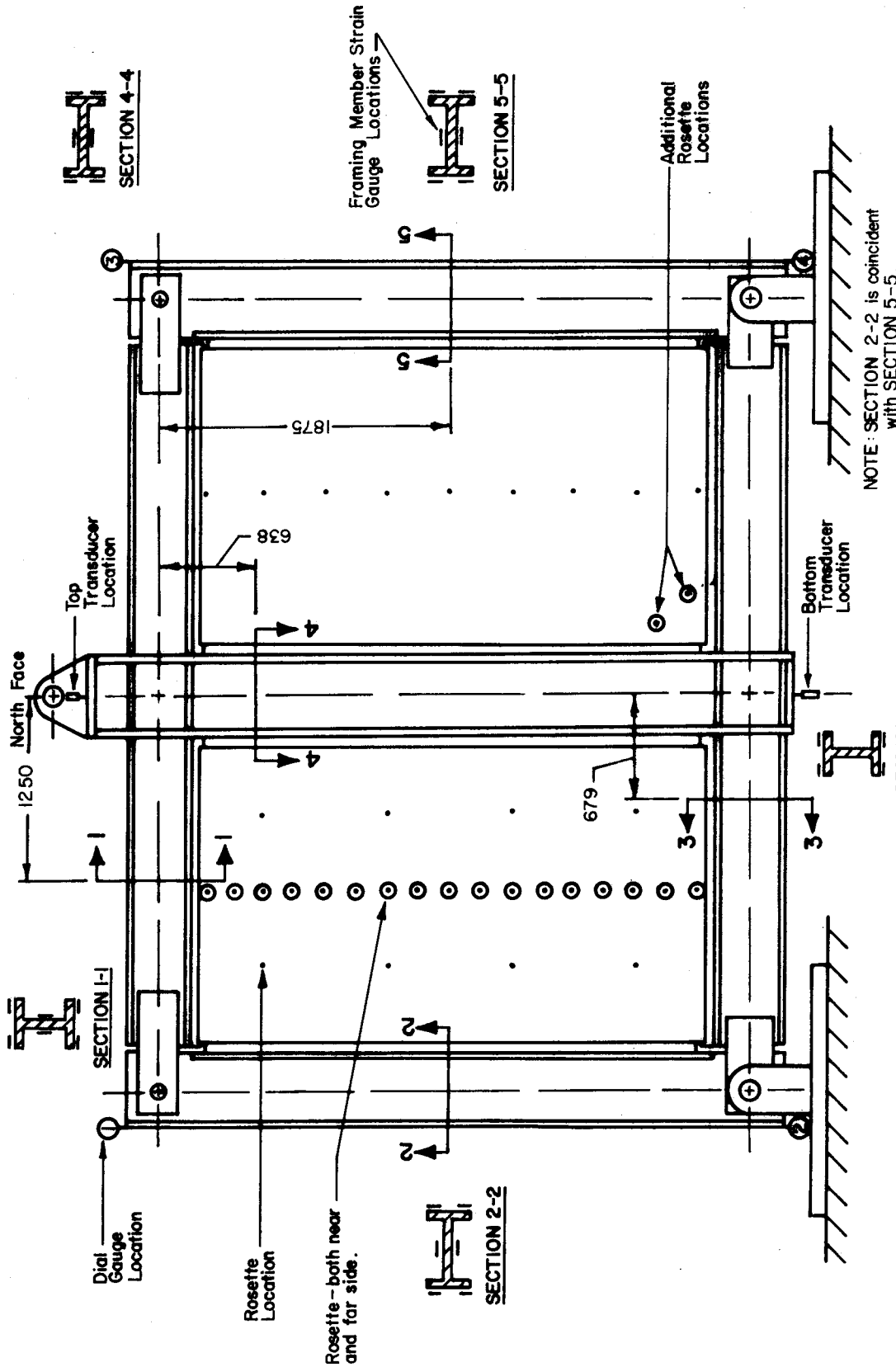

Figure 3.4 Gauge Locations and In-Plane Deflection Instrumentation

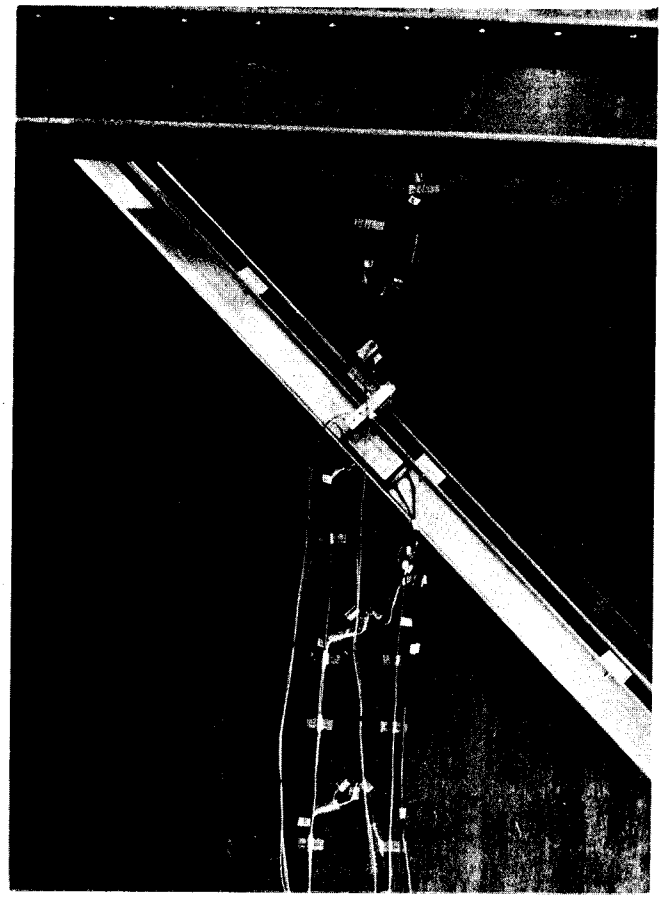

Figure 3.5 Orientation of Web Deflection Measurement Device

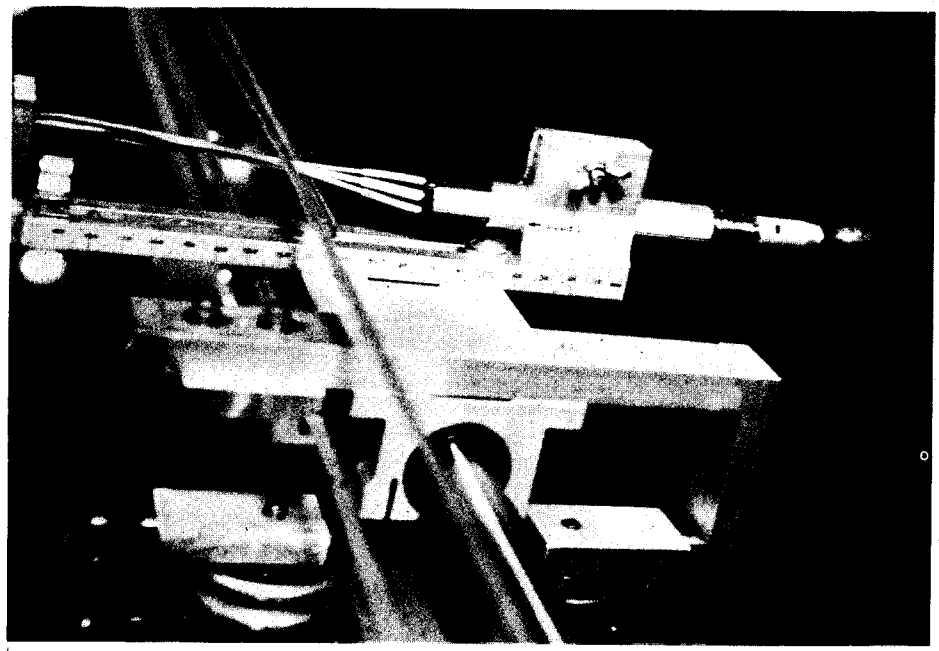

Figure 3.6 Close-Up of Web Deflection Transducer and Track

4. Test Results

4.1 Introduction

The results presented in this chapter reflect the findings of the experimental procedure previously described. A brief outline of the testing history of the program is listed in Table 4.1. Strain gauge results from Test #1 are omitted from this report because of problems with the electrical strain data acquistion at that time.

4.2 Coupon Tests

The averaged results of three static yield stress determinations per coupon test are summarized in Table 4.2. Each test exhibited a stress-strain relationship characteristic of a cold-worked plate. The value of 271 MPa is somewhat lower than the specified minimum yield strength of 300 MPa.

4.3 Full Scale Test to Service Loads

4.3.1 Web Plate Stresses

An examination of the surface stresses in each panel was made to determine whether the load distribution through the web plates was symmetric. Figure 4.1 indicates the magnitude and direction of the web plate principal surface stresses at the rosette strain gauge locations taken from a typical loading excursion to the serviceability deflection

limit. The stresses shown take into account the axial tension within the plate as well as the bending effects due to local plate buckling. At a few locations, where it is believed erroneous results were obtained because of faulty electrical equipment or poor bonding of the strain gauge, readings have been omitted.

By direct comparison between the stresses at identical locations on the other panels, it is seen that the general distribution of stresses between the two web panels is in agreement. The difference in direction between some of the principal stresses located on the centerline of Panel #1 as compared with the same gauge located on the back side of the plate (Panel #4), is explainable after examination of the locations of the buckles. Stresses are expected to be of contradictive sense, perpendicular to the formation of a buckle, on opposing sides of the plate. On one surface, the crest of a buckle creates a positively stressed region, whereas on the reverse face, a negatively stressed region is located in the trough.

To eliminate the bending stresses associated with the buckling of the web panels, the strains as obtained from both sides of the plate were averaged. The results, of the centerline gauges of Panel #1 were averaged with the gauges of Panel #4 and are presented in Figures 4.2 through 4.5 for Test #3.

One continuous hysteresis loading of the specimen to its serviceability deflection limit was performed two times

during this test. Because of the self weight of the specimen, approximately 41 kN, adjustment to the applied serviceability load (2104 kN) was made for both directions of loading. During the compression excursion, a service load limit of 2063 kN was used; in tension, a load of 2145 kN was applied.

Figures 4.2 and 4.4 represent the in-plane principal stresses within the web plate achieved upon application of the compressive serviceability load. The stresses reached during the tension service cycles are shown in Figures 4.3 and 4.5. Except for the second and third uppermost gauges, all the rosette locations exhibit agreement as to the general direction of the major (tensile in this case) principal stress. Furthermore, the overall trend appears to indicate that the tensile stresses are of the same magnitude. Comparison of Figures 4.2 and 4.4 shows that approximately the same level of stress is achieved for the first and second compression cycle loadings. Similarily, duplicate results were attained for the first and second tensile loadings as shown in Figures 4.3 and 4.5.

Figures 4.2 and 4.3, wherein the application of load is in the opposite sense, show that there is a region in the lower third of the panel where the major principal stresses differ somewhat in both magnitude and orientation for these two cases. The tensile web plate stresses present during the upward application of load were slightly larger and occurred at some lesser angle (with respect to the horizontal) than

those tensile stresses appearing during downward loading. In a similar fashion, there are larger tensile stresses in the upper region of the plate during downward application of load (Figure 4.2) than are present during upward loading. The angle of inclination of the tensile field as derived from the strain readings ranges between 44° and 56°. These values bound the predicted angle of 51.0° quite well.

4.3.2 Strains in Framing Members

The framing member strains for selected cross-sectional locations (see Figure 3.4) are presented for Tests #2 and #3 in Figures 4.6 through 4.9.

The strains as obtained from the tests were separated into their axial and bending components using the appropriate relationships. Examination of typical axial and bending strains (Figures 4.6 to 4.8) show that the strains were quite reproducible during the opposing cycles of loading of Test #3. Only a small amount of drift was apparent in the strain readings. For the most part, all the strains display a linear relationship with the applied load through to the serviceability load limit. For all cross-section locations, the slopes of the strains between compression and tension loadings are only marginally different. Strains obtained during the tensile portion of the cycled load for cross-sections 1, 2, 3 and 5 indicate that they are smaller than those achieved during compression loading. For cross-section 3 however, where the member is in tension during the

compression portion of the hysteresis, the strains are smaller.

Cross-sections 2 and 5 are identical locations on the two exterior representative floor beam members. With reference to Figures 4.6 and 4.8, there appear to be several differences between the strain results. During compression loading, the bending strains of cross-section 2 are smaller than the axial strains, whereas the opposite is true of cross-section 5. Furthermore, both the axial and bending strains are of greater magnitude at cross-section 5 than at cross-section 2. Examination of the tensile cycle portion of the bending strains at cross-section 2 indicates that the member bends inward, as it has for the compression cycle. From the strain readings at cross-section 5, however, the member bends outwards during tension loading. A small amount of bending is also present in the central beam member, as shown in Figure 4.7. Both of these effects seem to suggest a slight unbalance in the assumed equal load distribution between the two test panels.

Examination of the measured strains at the various locations generally showed good correlation between the results obtained during Test #2 and those from the primary cycle of loading of Test #3. (Both of these cycles were compression tests.) Figure 4.9 shows typical results. Correlation was not satisfactory at cross-section 3 where only four strain gauges were used as compared to six at all other locations.

4.3.3 Frame Deflection

The load-deflection histories of Tests #2 and #3 are presented in Figure 4.10. The hysteresis behavior of Test #3 demonstrates that the slope between identical load excursions is the same. The results as obtained from Test #2 agree well enough with the load-deflection slope of Test #3 during the compression loading. There is a larger frame displacement at the service load limit during the tension cycle loadings of Test #3 than experienced in all the compression test cycles. The increased deformation is a result of the elongation of the floor bolts under tension. A check of the uplift of the base plates at the service load limit verified that the difference between the deflection of opposing cycles was due to this effect. For all load applications, there is definite elastic behavior throughout the serviceability range. Upon unloading, some residual deflection is noted in each test. This was most likely the result of small deformations acquired in the reaction tongues during both cycles of loading.

4.3.4 Web Plate Deflection

Information was gathered on all out-of-plane web deflections, as measured on a cross-section perpendicular to the expected direction of the tension field formation. The maximum relative out-of-plane deflection of the web plate at service loads for Tests #1, #2 and #3 are summarized in Table 4.3. All measured deflections are reported with respect

to a hypothetical perfectly flat web plate.

Figure 4.11 shows the complete behavior of the web plate during the entire tensile load history of Test #1. There was a gradual progression in magnitude of the buckles as the loading was increased. When unloaded, the web plate returned almost identically to its original state, thereby indicating no permanent set or deformation. This is shown by the dashed curve superimposed on the zero loading state.

Figure 4.12 shows the zero and maximum service load deflections for Test #2, a compression test. The initial profile of the plate is different from that shown in Figure 4.11 for the tensile test because the cross-section here is perpendicular to that of Test #1. Again it is noticed that the plate returns to its original position upon unloading. During this test, a small amount of flaking of whitewash occurred at the service load limit near the upper exterior corner of the web plate of Panel #3. Measurements taken of the yielded portion indicated that the angle it had formed at was about 44°. This yielding probably occurred as a result of the poor detailing at the web plate to fish plate junction in the corners. Stiffening of the corner connections was made prior to proceeding with the next test.

In Test #3, the web deflections were examined only during the compression cycles. As shown in Figure 4.13, nearly identical behavior between the two loading cycles was achieved. The maximum relative displacement during the second cycle is only marginally greater than that experienced

during the first. It is apparent that there is elastic behavior of the plate in all the tests.

It was noted that the buckles that had formed over a wide area of the plate, at both extremes of the load limit, were barely discernible to an observer standing only a short distance away from the specimen.

4.4 Full Scale Test to Ultimate Load

4.4.1 Definition of Limits

Both web stresses and framing member strains at two limits are examined in the following sections. These limits are the load corresponding to the end of linear frame behavior and the ultimate load. The linear load limit described in this report constitutes the calculated load that terminates the linear load-deflection behavior within the structure. This corresponds to first yield in the web plate. Once the plate begins to yield, non-linear deflection of the frame commences. The ultimate load of a framing scheme is defined as the highest load attainable prior to the eventual system collapse. For the frame tested, loading was applied incrementally until failure in a connection occurred, resulting in a subsequent load drop-off.

4.4.2 Web Plate Stresses

The averaged stress results from Test #4 for Panel #1 at a load close to the expected linear limit are presented

in Figure 4.14. The results obtained from the additional rosettes placed at the lower interior corner of Panels #2 and #3 were not considered reliable and they are therefore not included in this examination.

As before, many of the gauges agree as to the general direction of the principal stresses. The overall magnitude and distribution of stresses with respect to each other appear to be the same as experienced at the compressive service load levels of Test #3, that is, the stress distribution is generally uniform throughout the plate's gauged centerline. The stresses taper off to slightly lower levels near the ends. The direction of the principal stress associated with each gauge location does not change appreciably except for a few instances, and then only slightly, as compared to those angles attained at service load levels. Only the second and fourth rosette locations from the top give questionable results as they show both principal stresses as being positive. Many of the tensile stresses within the plate are in the range of 271 MPa, the yield strength of the material.

With reference to Figure 4.15, the web plate stresses achieved at ultimate load, the same pattern of stress distribution is again experienced. However, at this load stresses much higher than the yield stress are indicated in the web plate. Greater compressive stresses also occur in the central region of the plate. (In this report, the material response has been idealized to be that corresponding to

a tension test and only elastic, perfectly plastic regions are assumed. In reality, the plate material has some compressive stress perpendicular to the tensile stress, and also has a strain-hardening component.) Questionable results are again obtained in the upper portion of the plate where the stresses are quite high.

4.4.3 Strains in Framing Members

Figures 4.16 through 4.20 present the framing member strains for Test #4 at the five cross-sections located throughout the frame. The linear behavior of cross-sections 1, 2 and 3 (Figures 4.16, 4.17, 4.18) is bounded by loads moderately above the serviceability load limit. However, cross-sections 4 and 5 exhibit a much higher limit to the linear behavior, as shown by Figures 4.19 and 4.20. For cross-sections 1, 2 and 3, the bending strains increase much more rapidly than the axial strains following attainment of the linear limit.

The same inconsistencies between the identical cross-sections 2 and 5 that were observed in Tests #2 and #3 are also apparent throughout most of Test #4. Again, both the magnitude of the strains is smaller, while showing the axial strains to be greater than the bending strains at cross-section 2 as compared to cross-section 5. Very low bending strains occurred at cross-section 4, as was expected.

4.4.4 Frame Deflection

The overall frame behavior for the final loading test to failure is shown in Figure 4.21. The linear portion of the curve presents much the same slope as shown in the compression cycles of Test #3. The load corresponding to the limit of linear behavior is approximately 3400 kN. This is well above the serviceability load (2063 kN) for this frame. A gradual decrease in the stiffness was experienced beyond the linear load limit with very ductile behavior shown until the ultimate load of 5395 kN was achieved. The ultimate load was reached when a weld tear occurred at the web plate to fish plate connection located at the top pin-connection of Panel #2 (Figure 4.22). This was followed by buckling of the doubler plates at the same location and further weld tearing at a load of 5395 kN. It is likely that the ultimate load attained in this test, as governed by the failure of the detail, did not constitute the true ultimate load of the frame (web plate and bounding members).

4.4.5 Web Plate Deflection

The out-of-plane web deflections recorded for Test #4 are shown in Figure 4.23. The maximum relative out-of-plane displacement recorded was approximately 41 mm, attained at a load of 4968 kN. Loading during Test #4 was increased until this load was reached, at which point the stroke of the MTS testing machine loading ram was exhausted. (The specimen was then unloaded and a web deflection reading at zero load was

taken to assess the permanent deformation. It was decided not to place the web deflection measurement device back on the specimen for additional load increments since the ultimate load was close and a sudden failure could have damaged the equipment.)

Measurements taken along the crests of the major buckles that had formed on the south face of Panels #1 and #2 gave values of α between 46° and 53°. A large yield band had formed in each of the troughs of the buckles (north face) commencing at the top outside corners of Panels #3 and #4. These bands were inclined at about 44°. It must be recognized that considerable judgement was involved in measuring the angles of the buckles and yield bands.

Table 4.1 Full Scale Specimen Test History

Test #	Test Description
0	Preliminary tension test to check strain gauge response. (max. load=1100 kN)
1	First tension loading to full service limit. (max. load=2145 kN)
2	First compression loading to full service limit. (max. load=2063 kN)
3	Double hysteresis loading to full service limits. (max. loads=2145 kN and 2063 kN)
4	First attempt to ultimate load in compression. (max. load=4968 kN)
5	Continuation of ultimate test in compression. (max. load=5395 kN)

Table 4.2 Coupon Test Results

Coupon Test #	Static Yield (MPa)	Avg. Static Yield Per Test (MPa)	Total Avg. Static Yield (MPa)
1	260.5 268.4 278.9	269.3	
2	271.1 275.0 273.7	273.3	270.8
3	264.5 271.6 273.7	269.9	

Table 4.3 Web Deflection Summary at Service Loads

Test #	Loading Type	Initial Out-of-Flatness (mm)	Over a Length of Appox. (mm)	* Max. Relative Defl. (mm)
1	tens.	9.4	2000	15.8
2	comp.	8.8	1550	19.8
3	comp. comp.	8.8 9.2	1275 1275	19.8 19.8

* Maximum relative deflection with respect to a perfectly flat web plate.

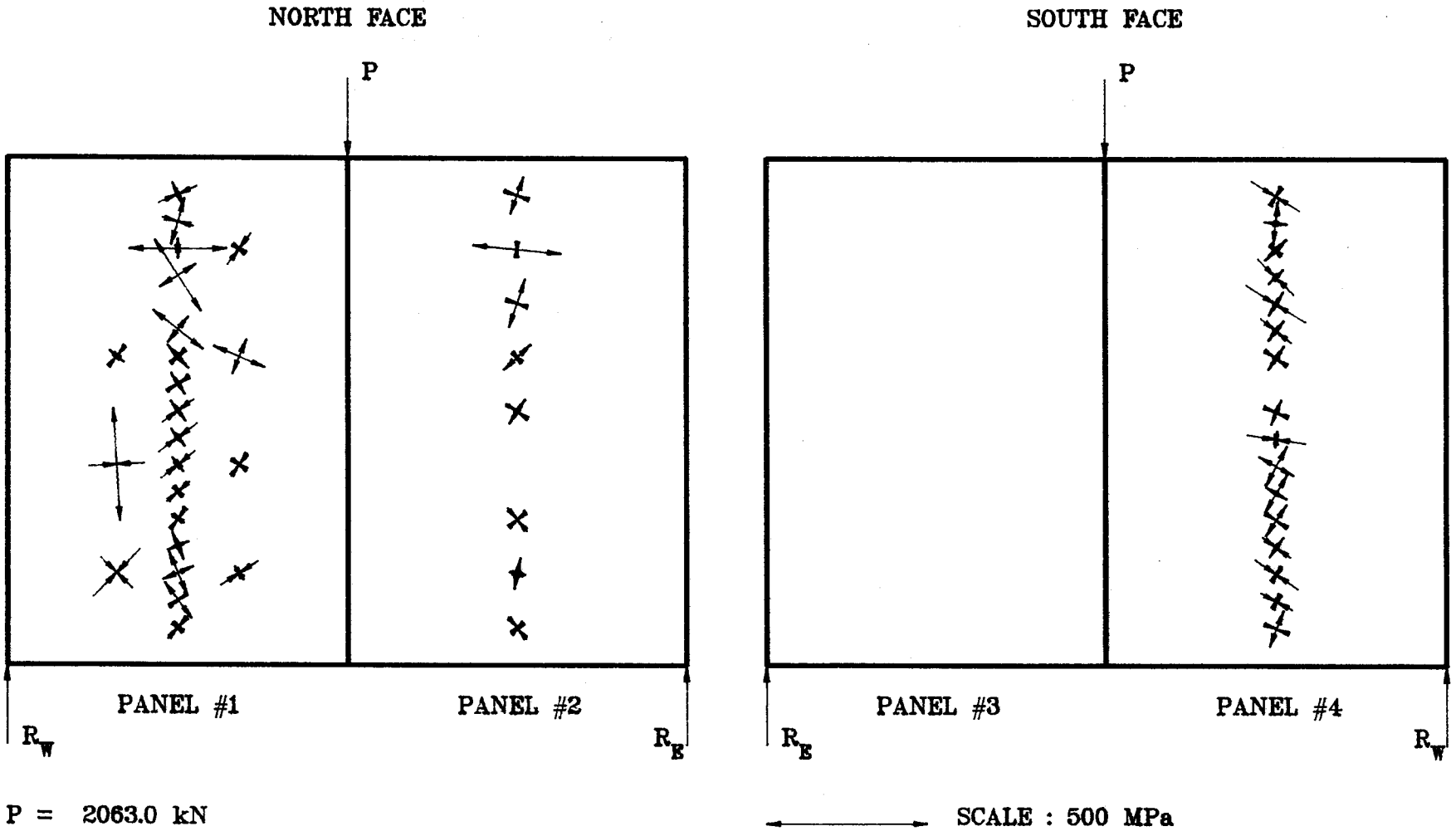

Figure 4.1 Unaveraged Principal Stress Readings, Test #3

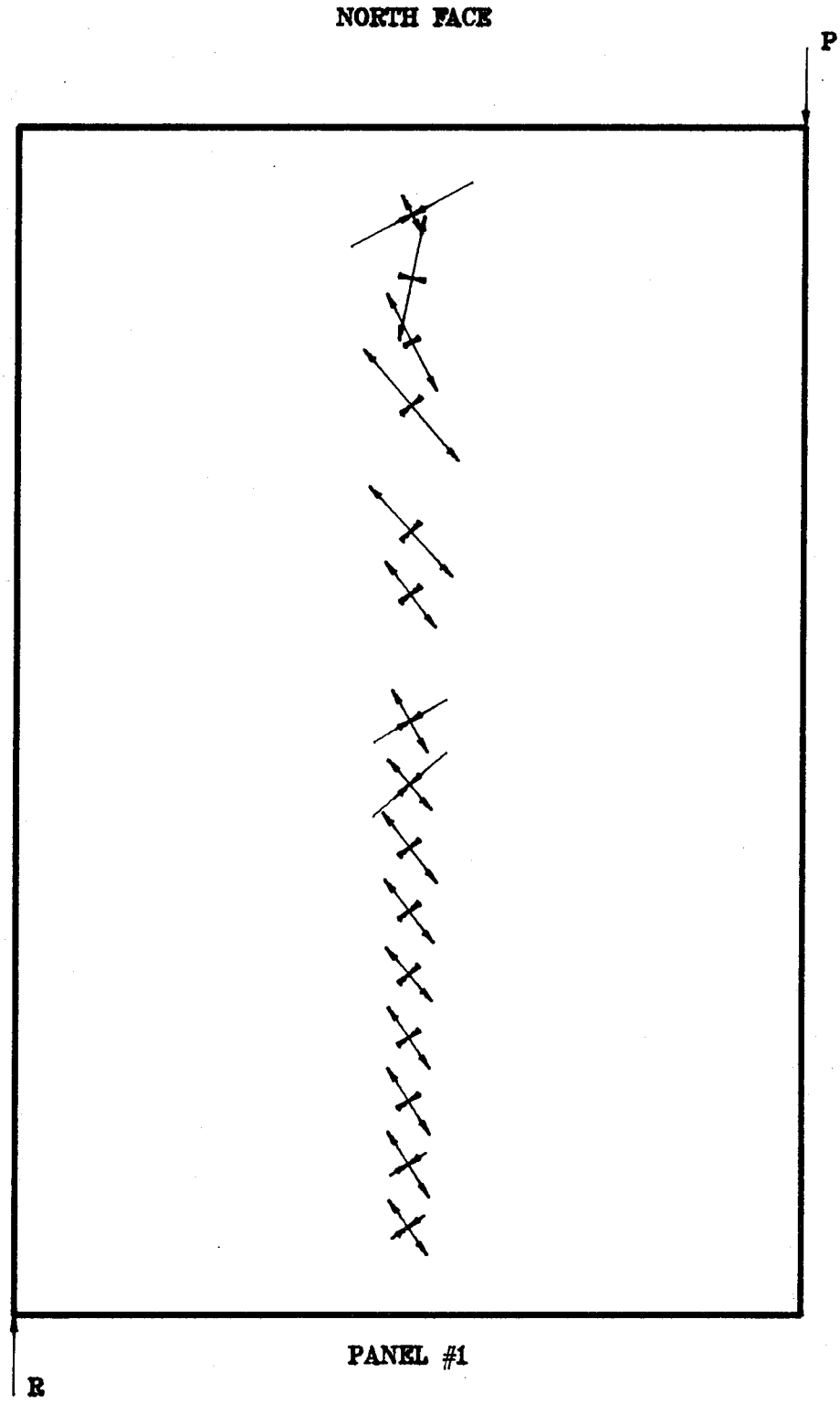

Figure 4.2 Averaged Principal Stresses, 1st Comp. Cycle, Test #3

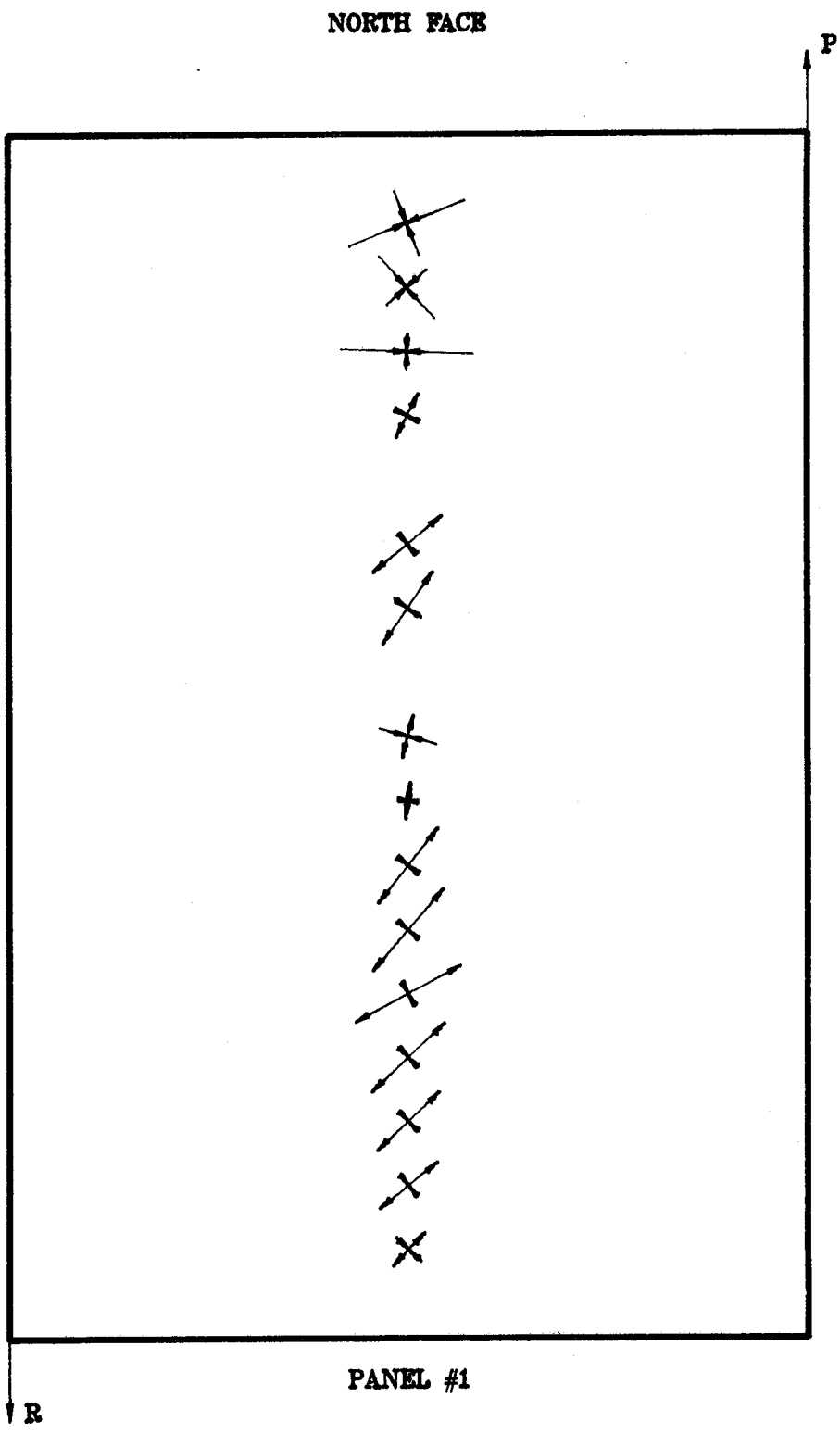

Figure 4.3 Averaged Principal Stresses, 1st Tens. Cycle, Test #3

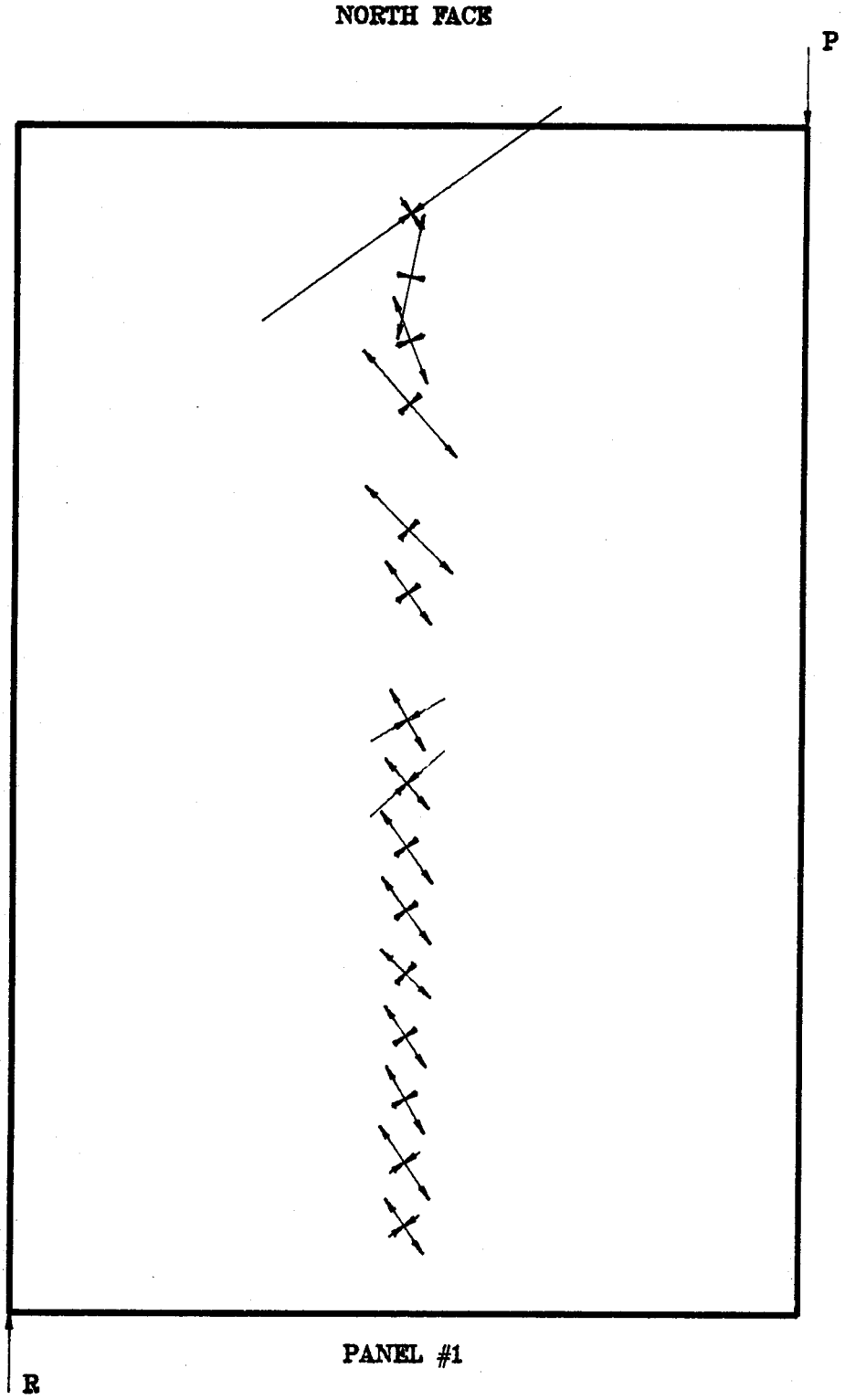

Figure 4.4 Averaged Principal Stresses, 2nd Comp. Cycle, Test #3

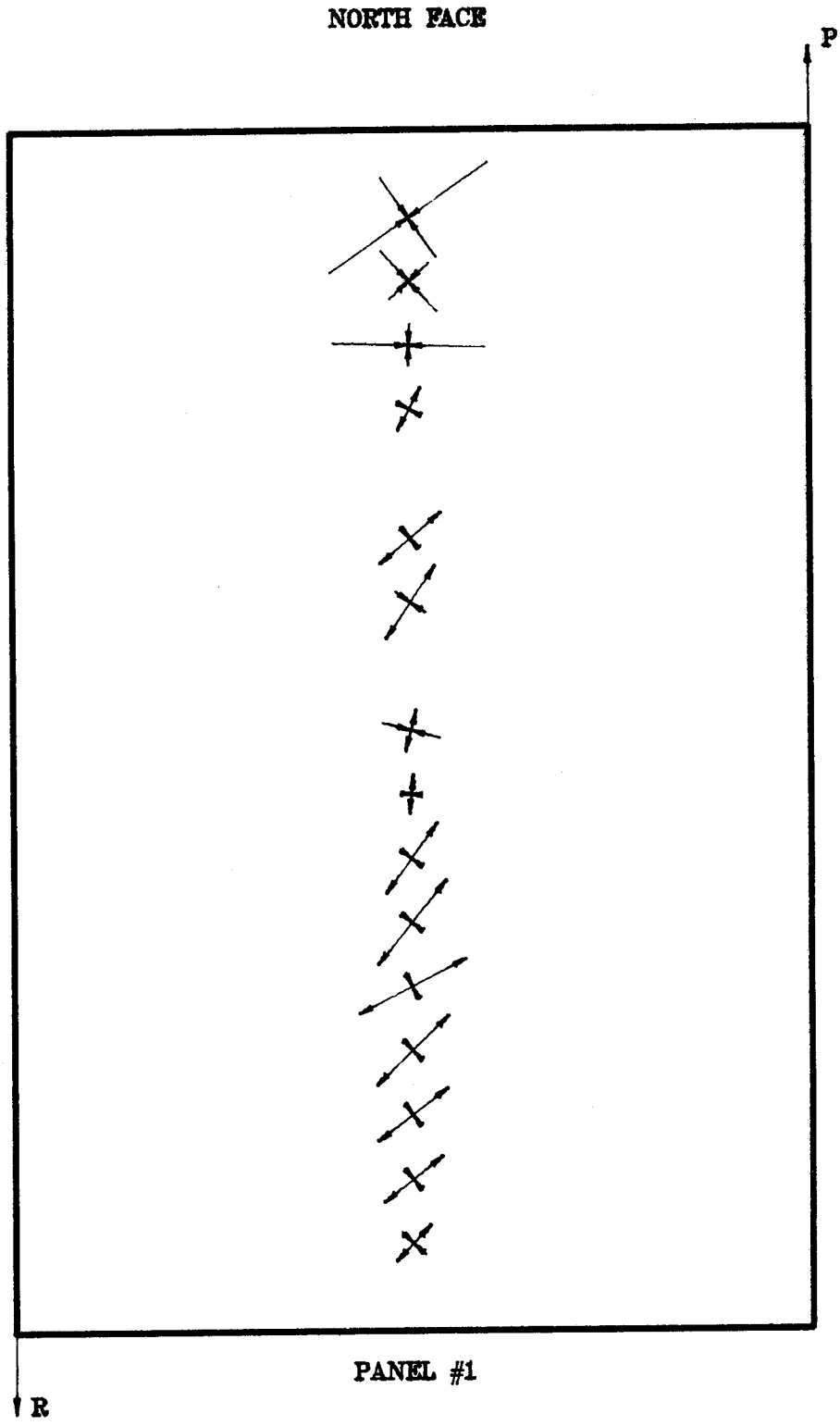

Figure 4.5 Averaged Principal Stresses, 2nd Tens. Cycle, Test #3

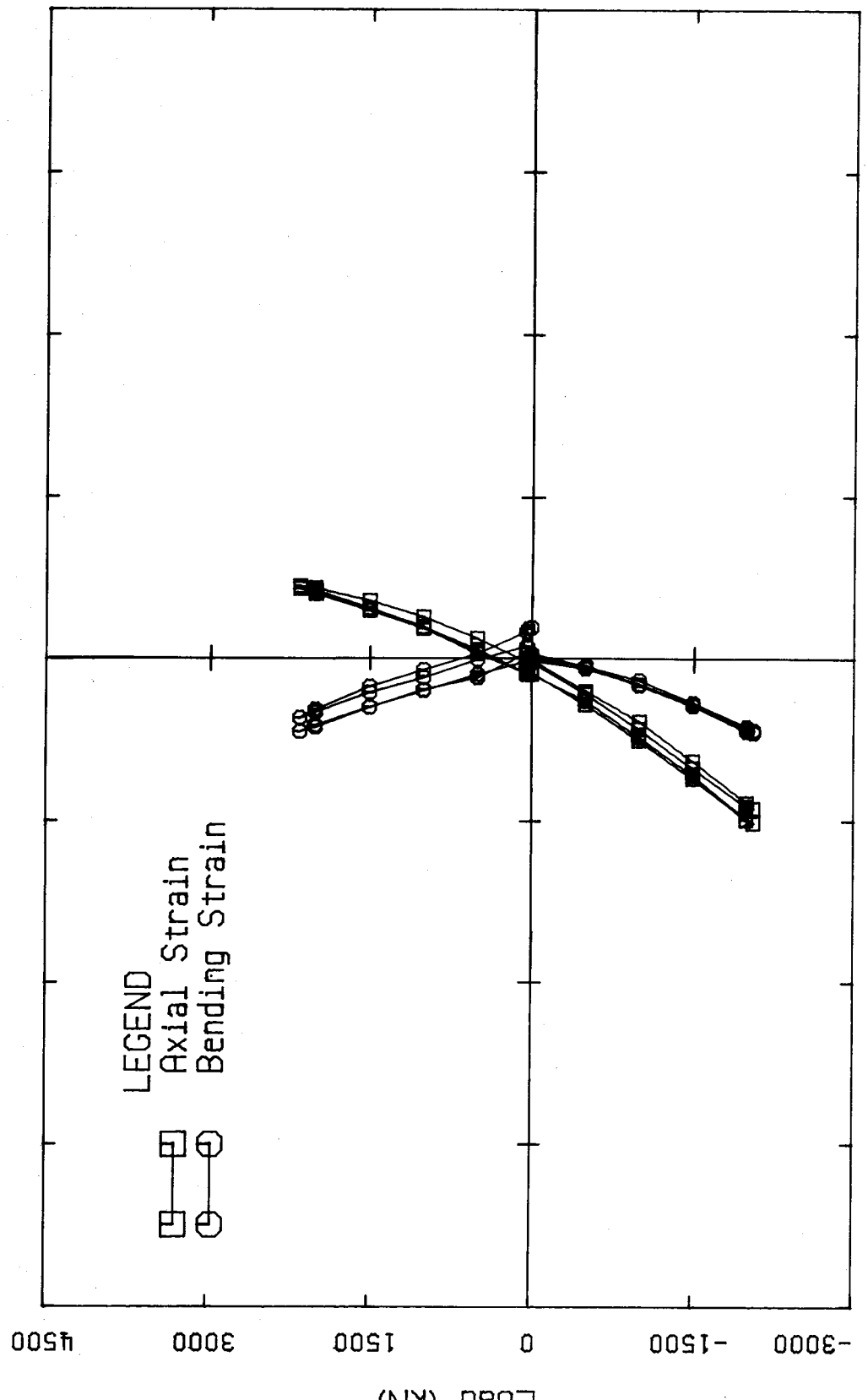

Figure 4.6 Section 2 - Axial and Bending Strains, Test #3

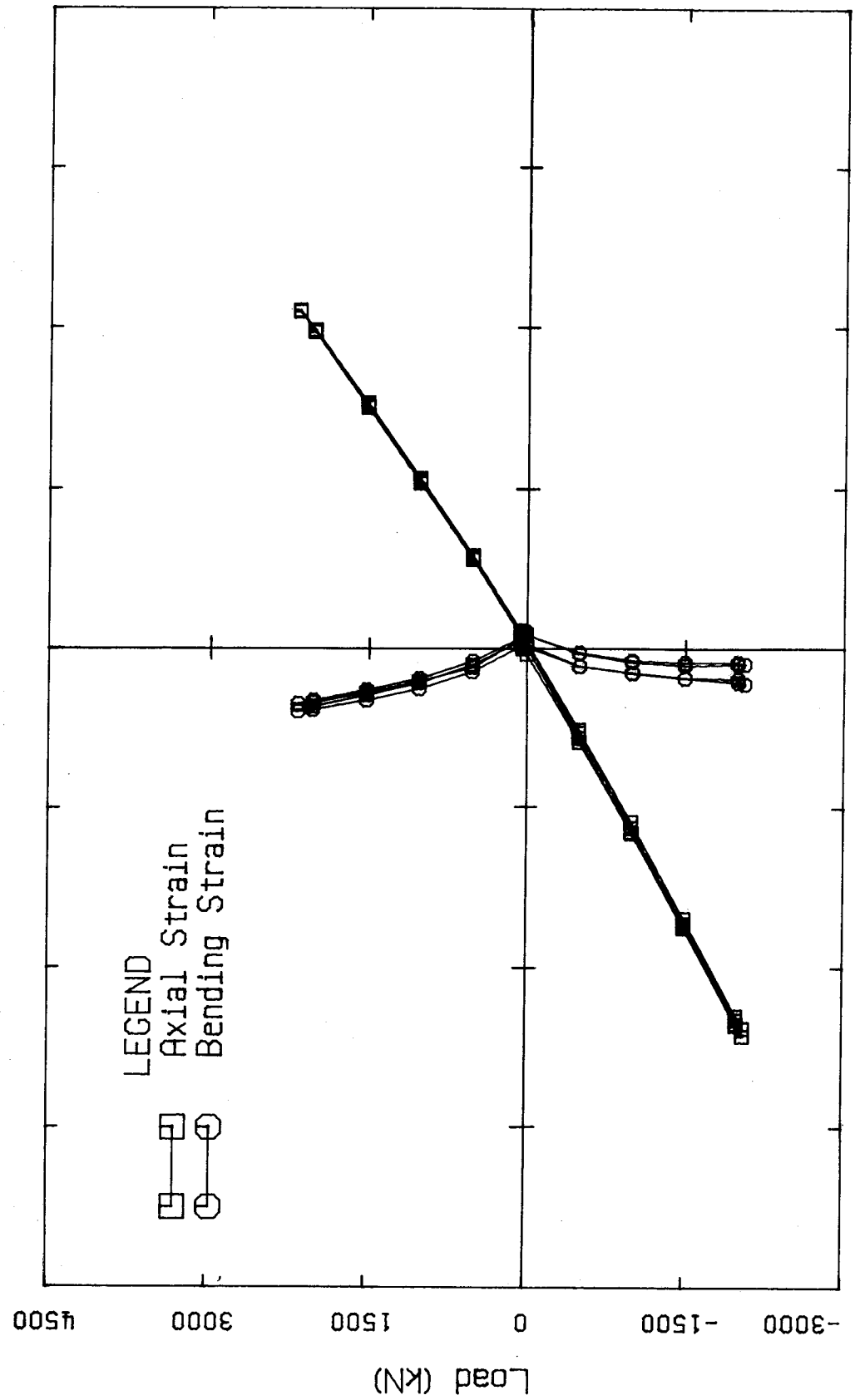

Figure 4.7 Section 4 - Axial and Bending Strains, Test #3

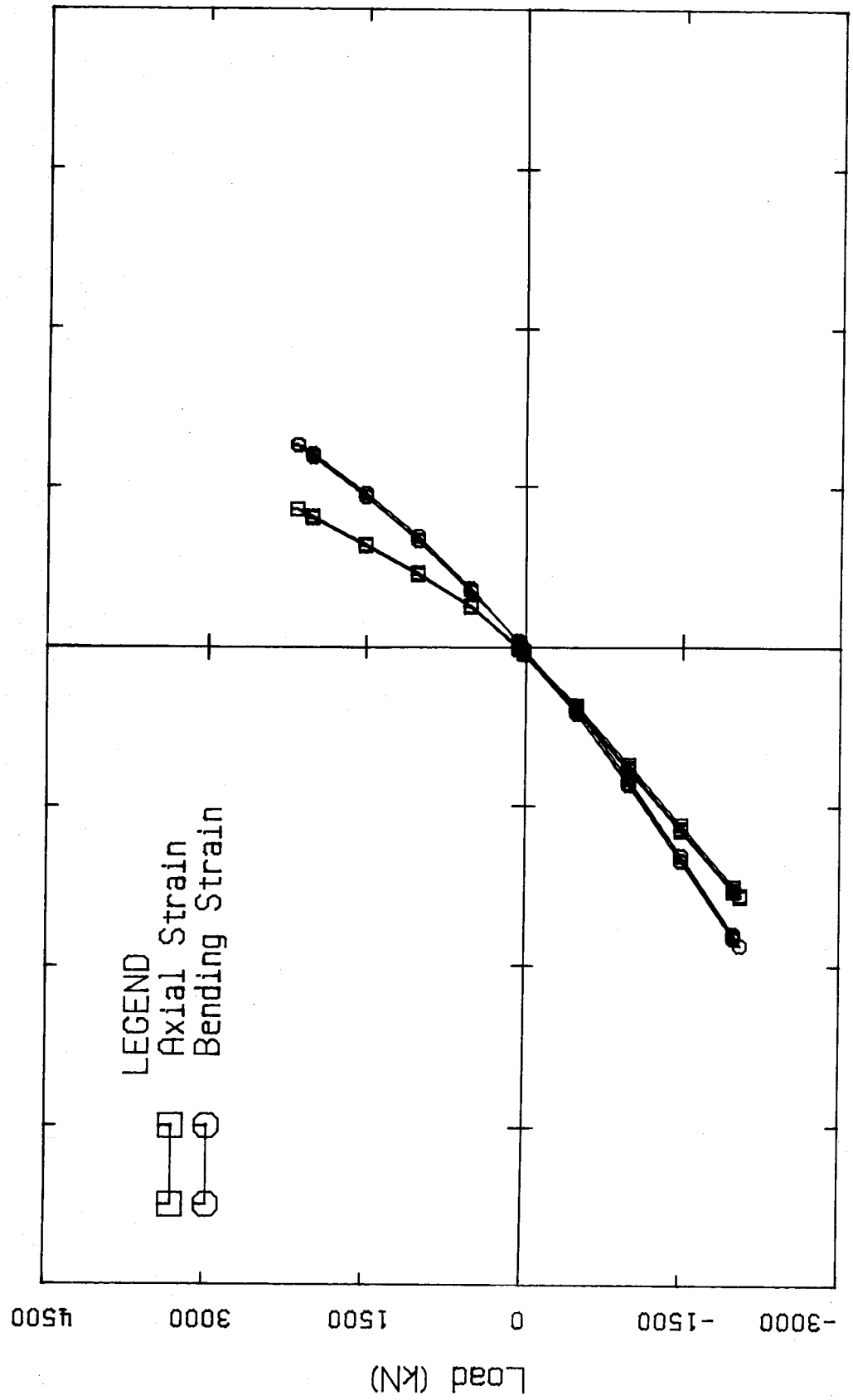

Figure 4.8 Section 5 - Axial and Bending Strains, Test #3

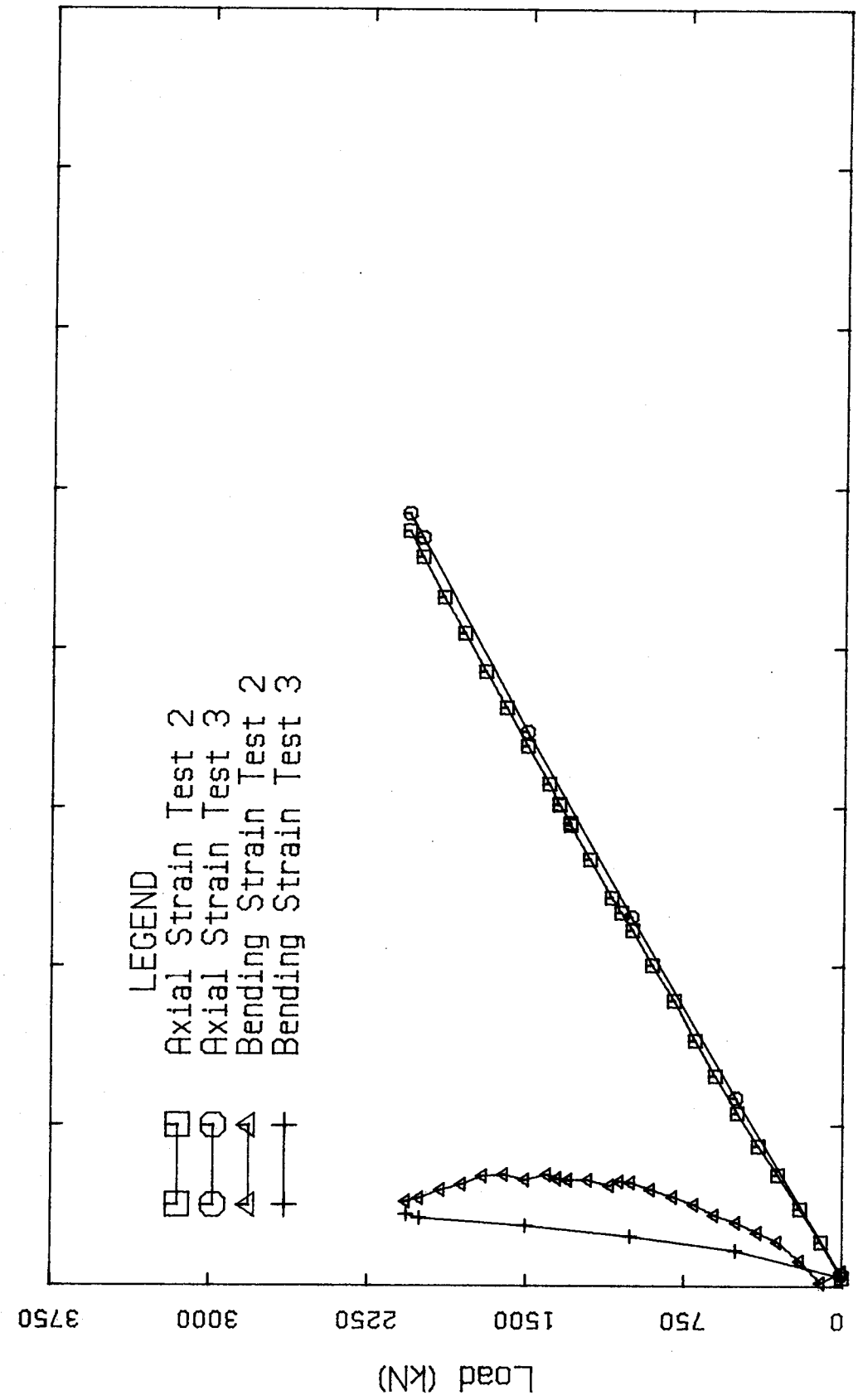

Figure 4.9 Section 4 - Absolute Strains, Tests #2 and #3

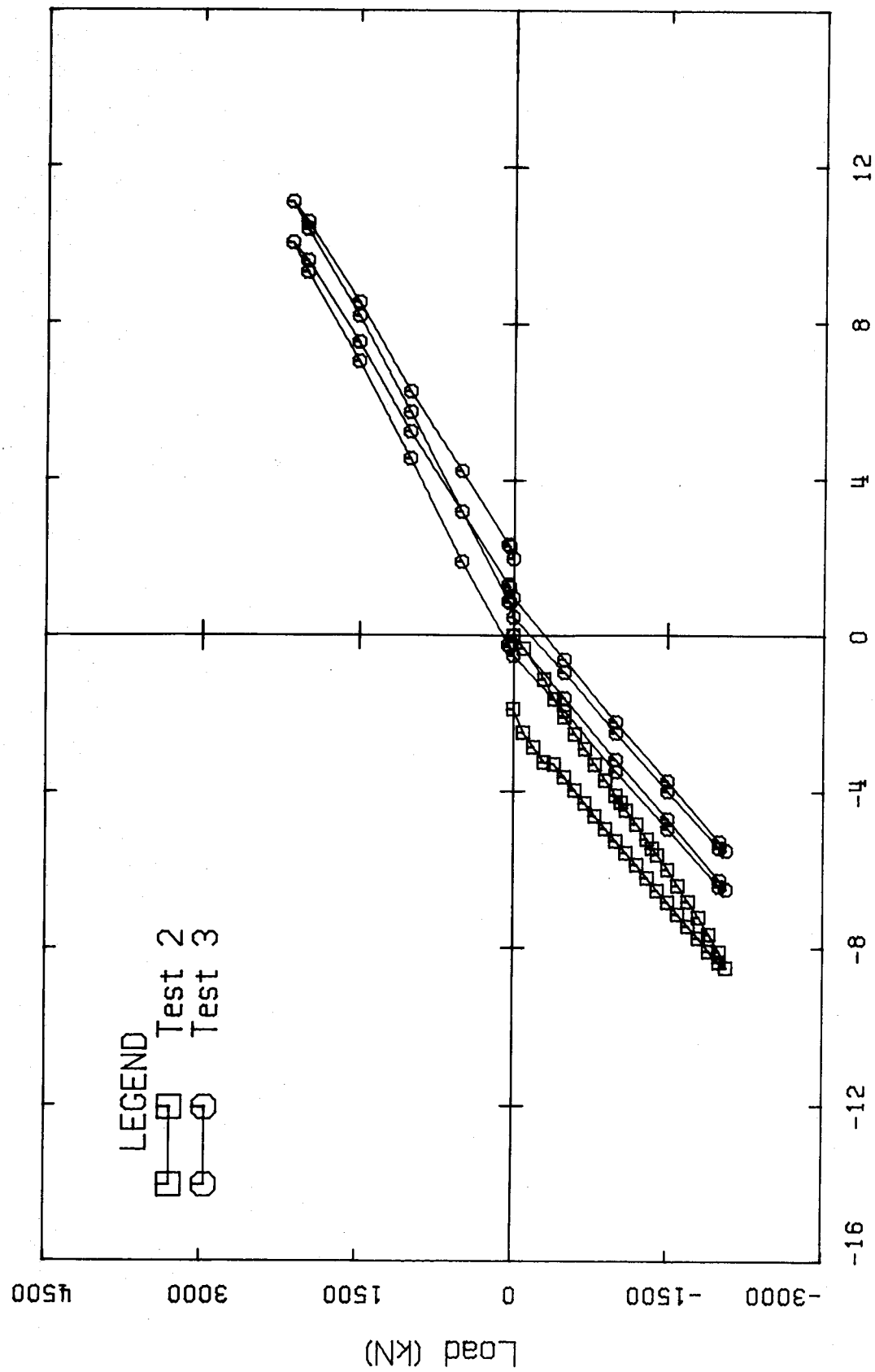

Figure 4.10 Load vs Deflection, Tests #2 and #3

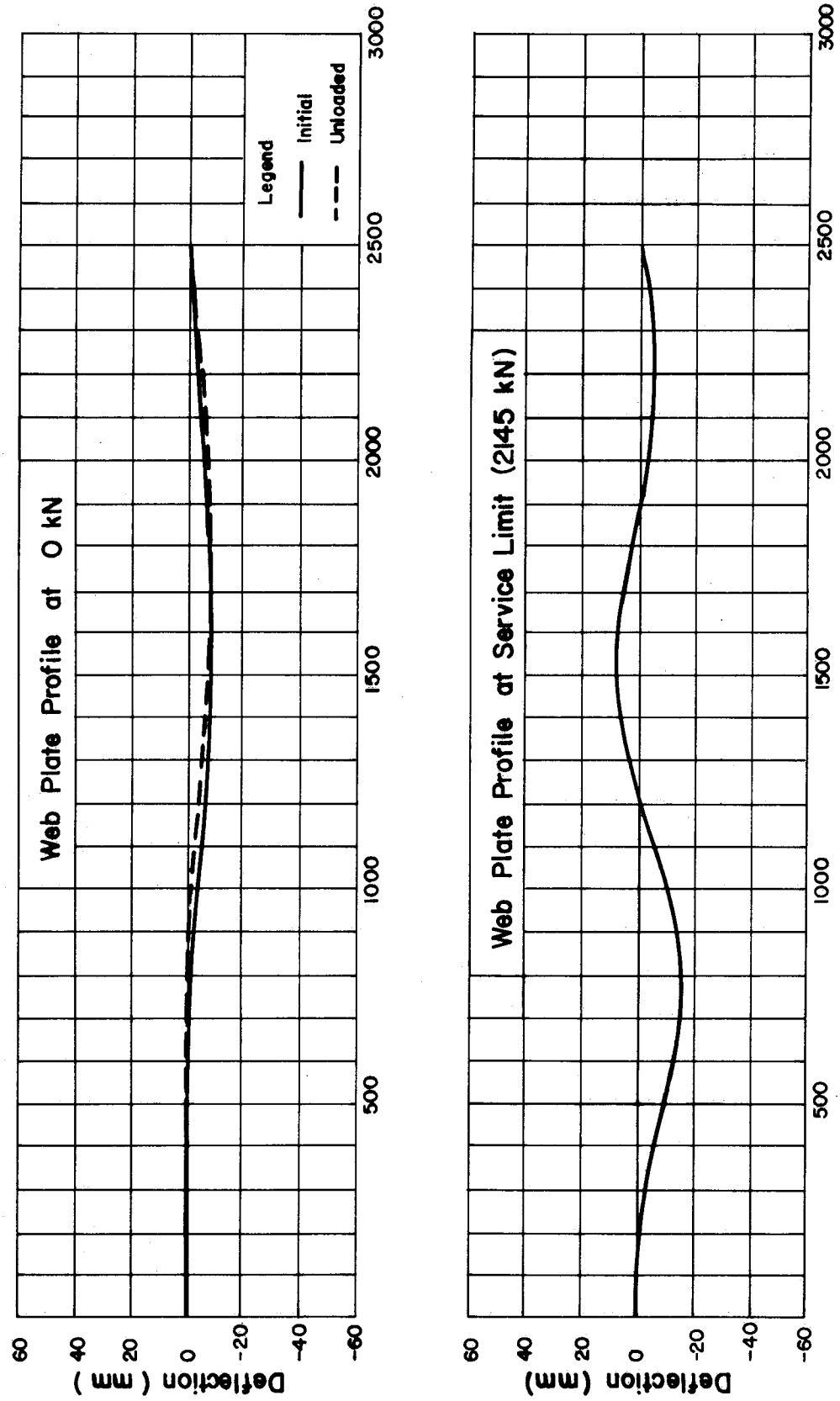

Figure 4.11 Web Deflection, Test #1

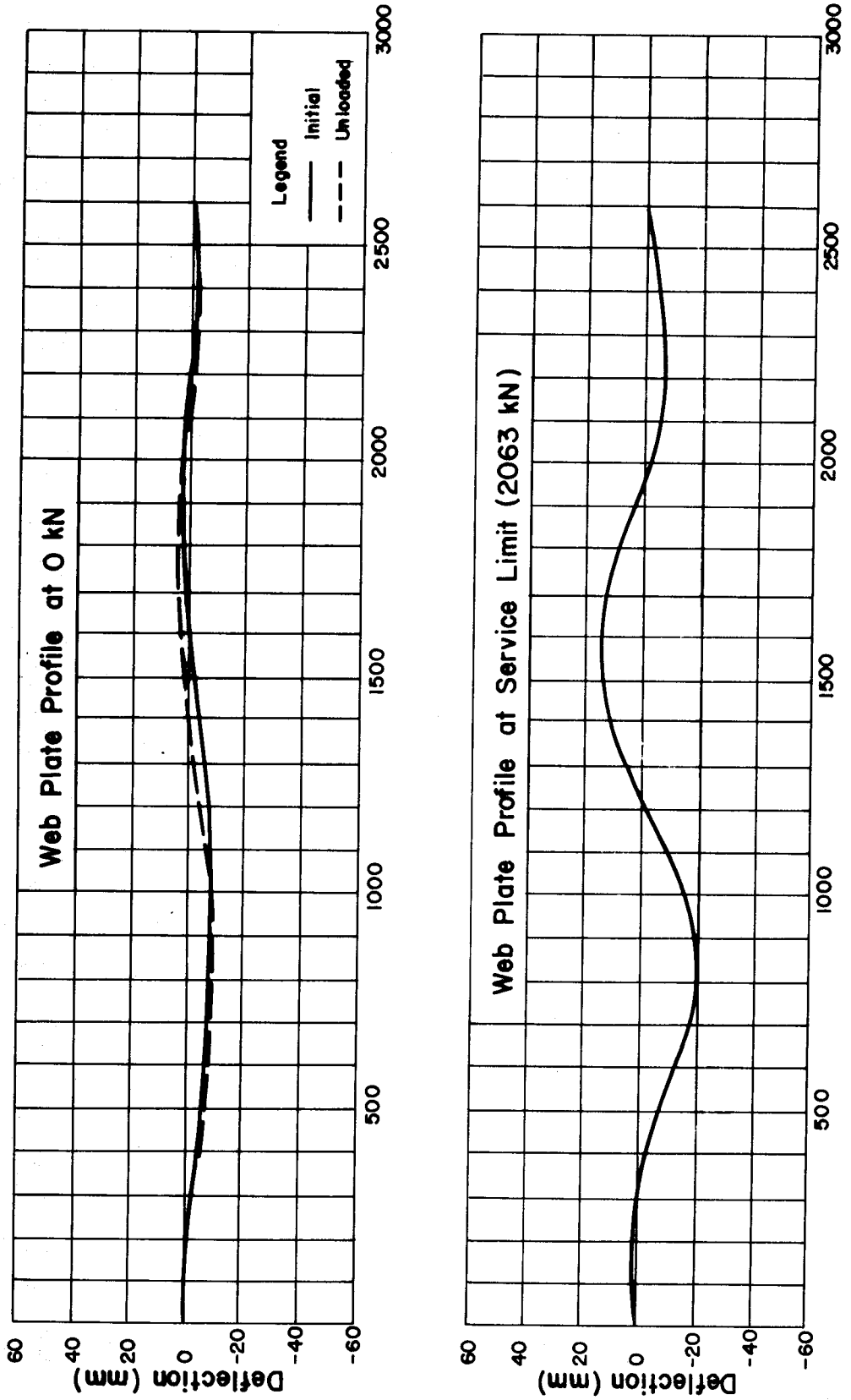

Figure 4.12 Web Deflection, Test #2

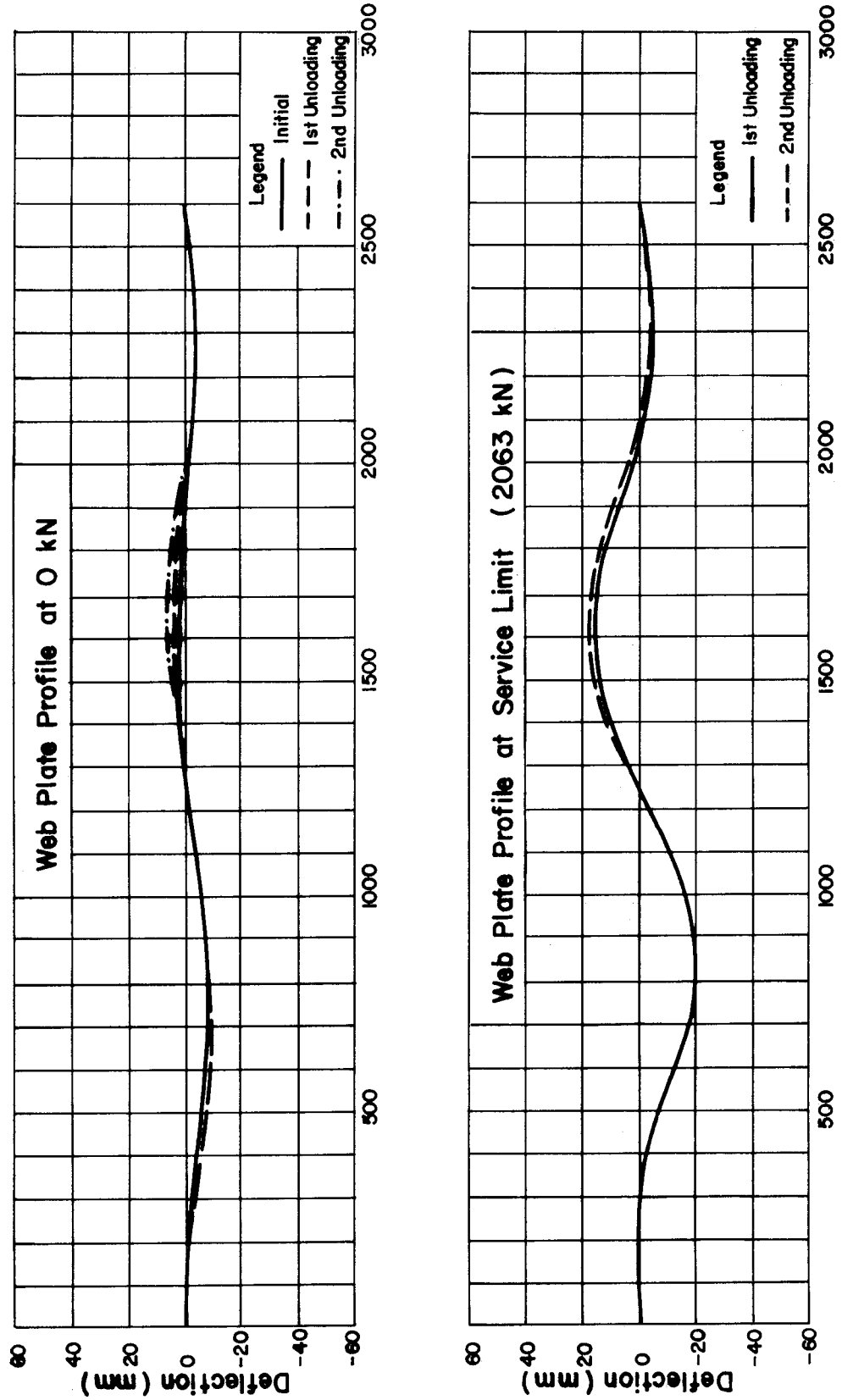

Figure 4.13 Web Deflection, Test #3

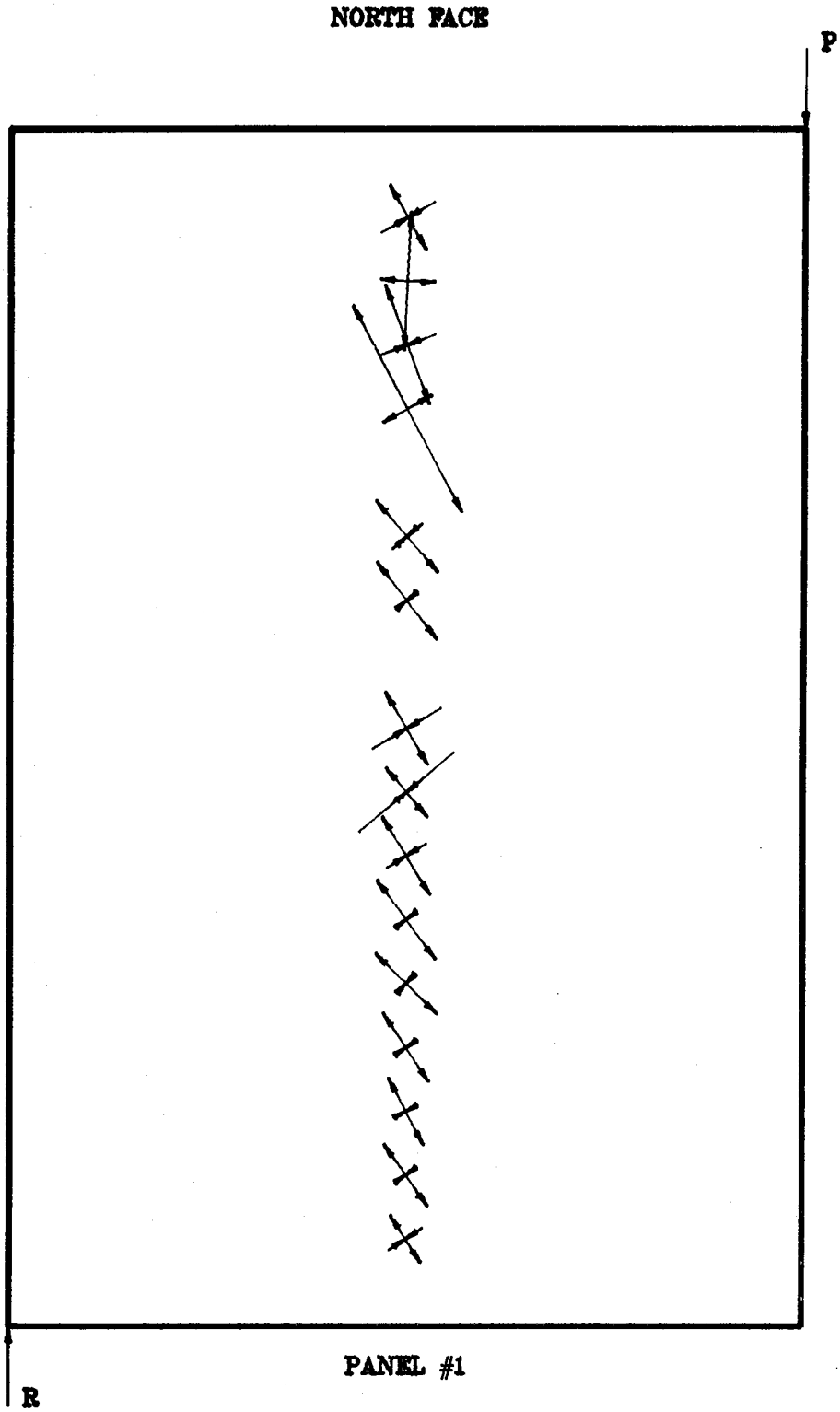

Figure 4.14 Averaged Principal Stresses, First Yield, Test #4

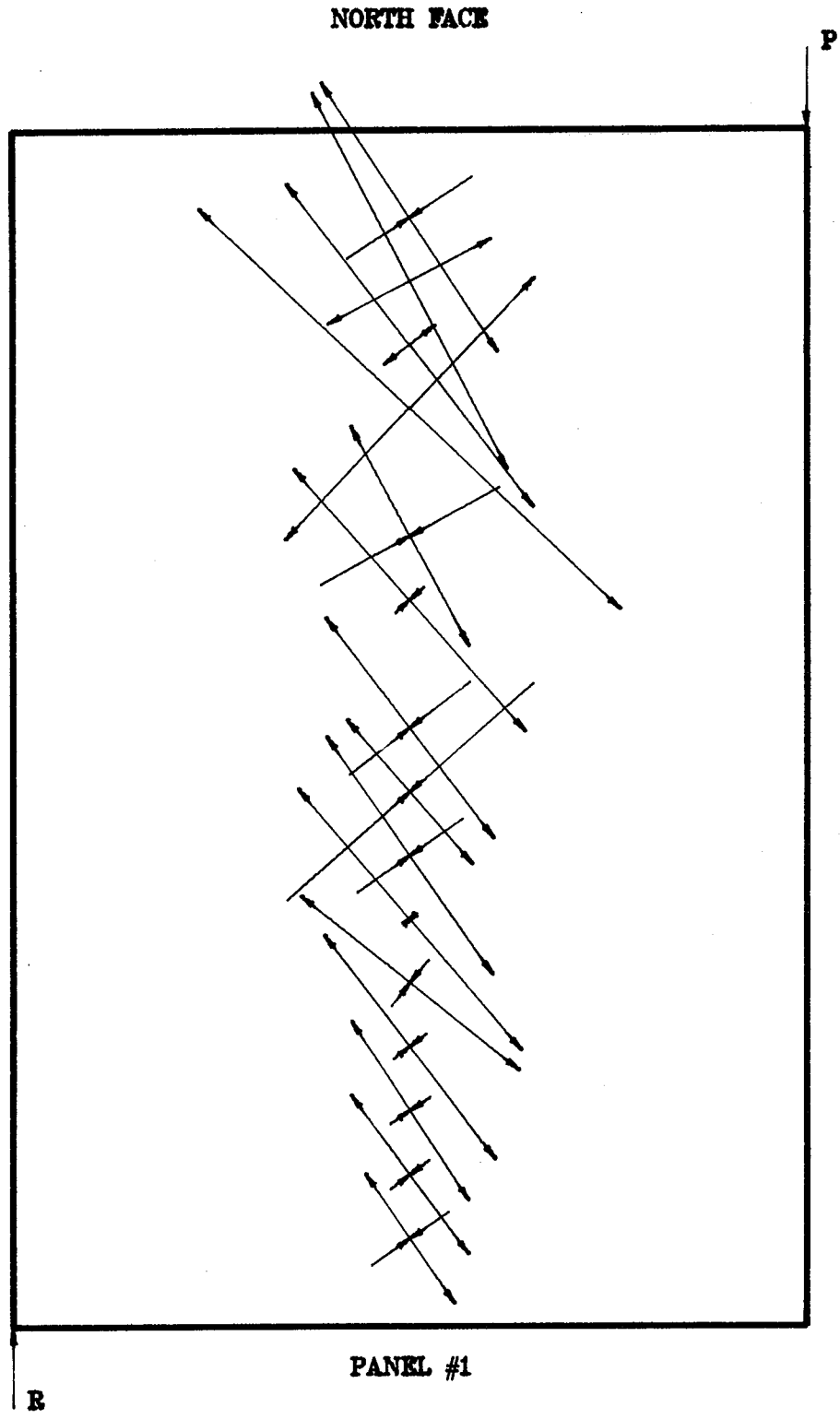

Figure 4.15 Averaged Principal Stresses, Ultimate Load, Test #4 - #5

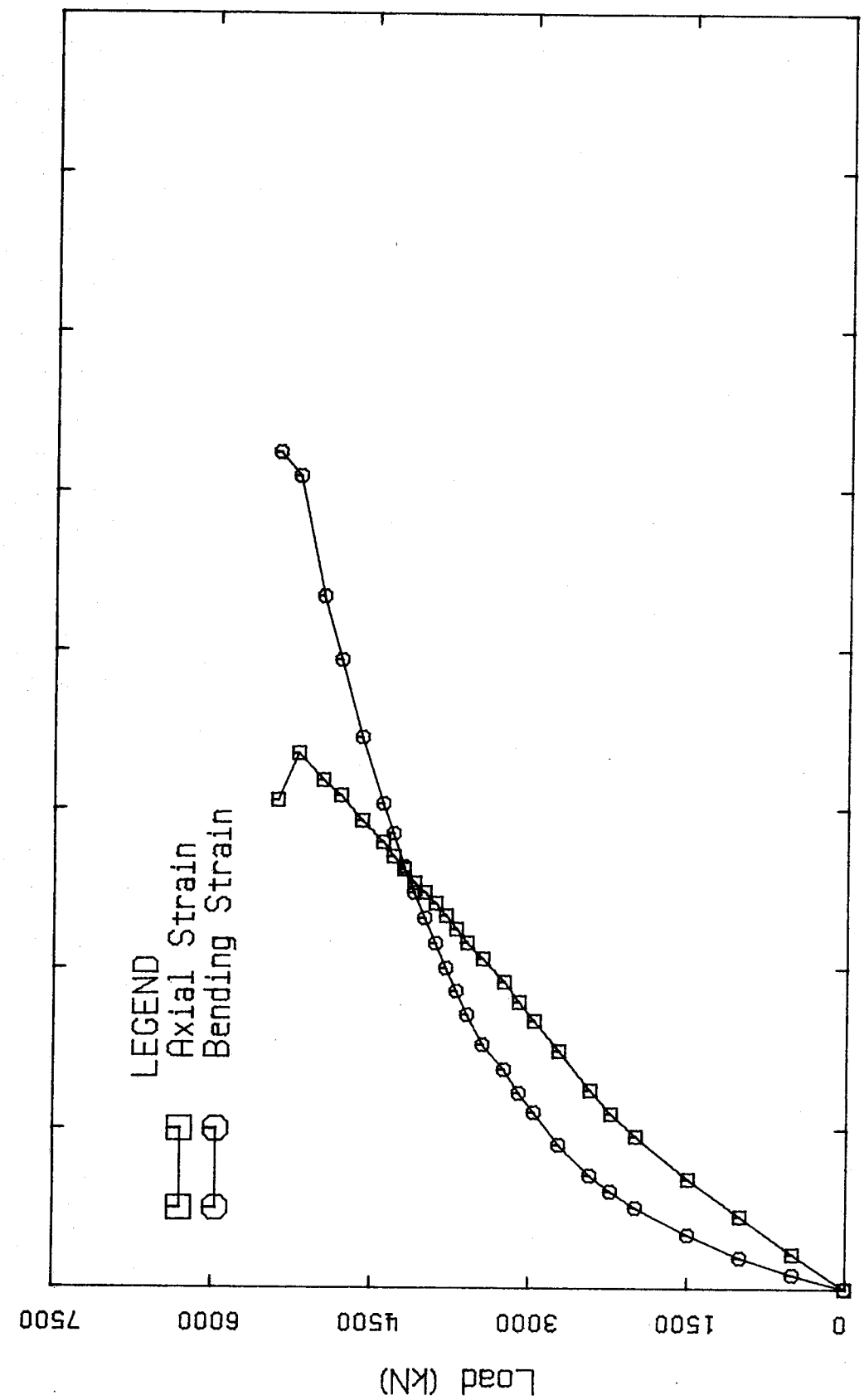

Figure 4.16 Section 1 - Absolute Strains, Test #4 - #5

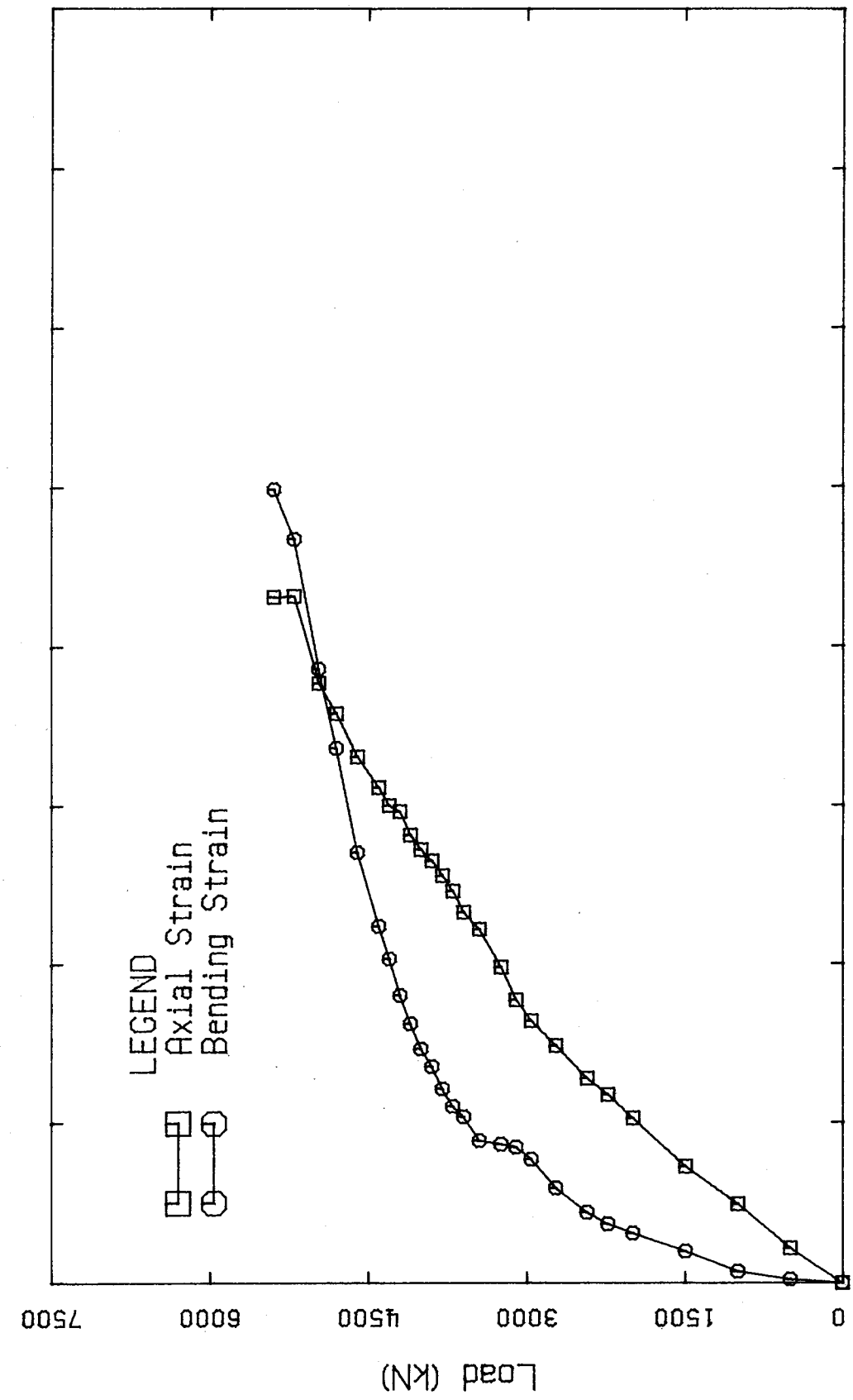

Figure 4.17 Section 2 - Absolute Strains, Test #4 - #5

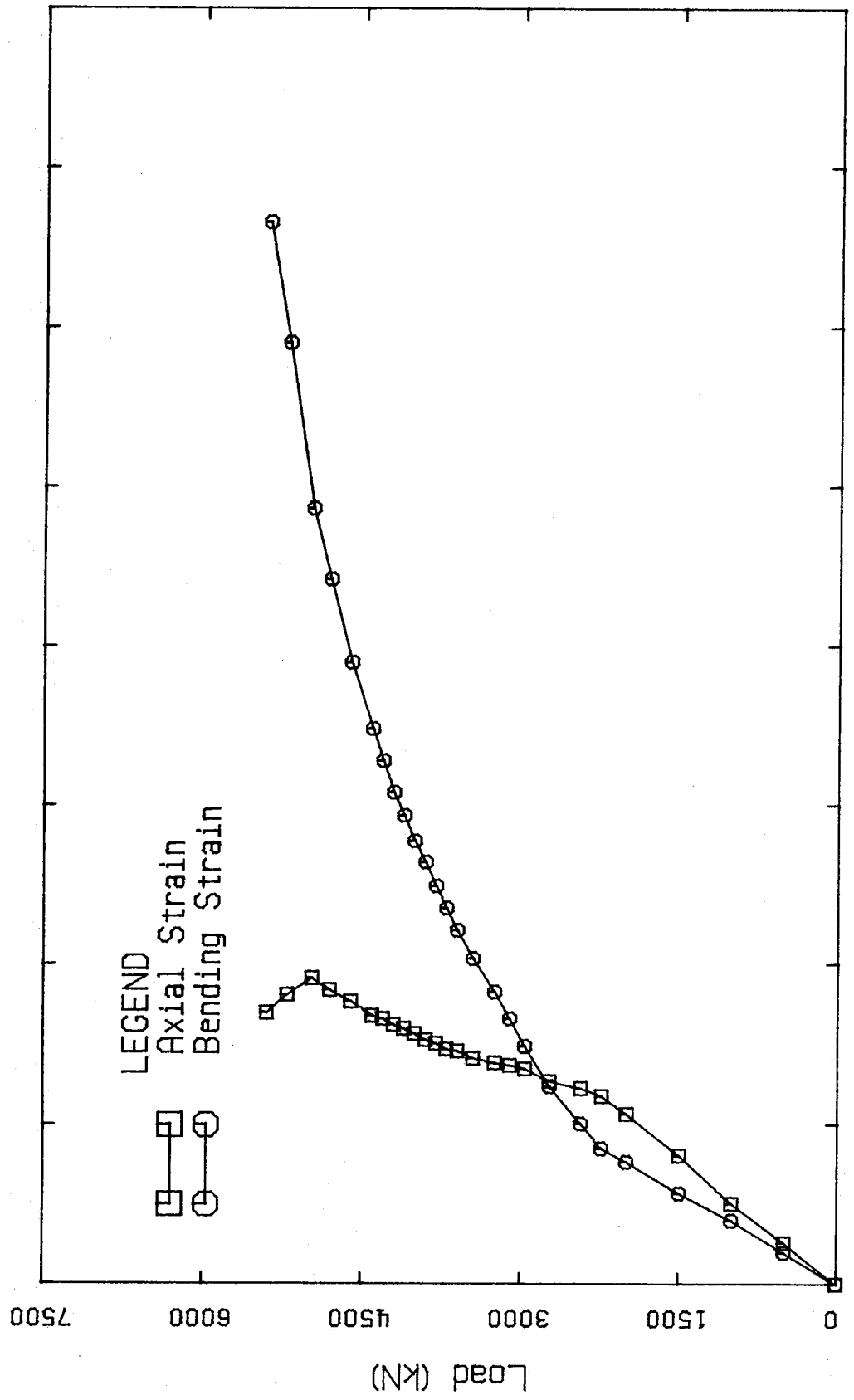

Figure 4.18 Section 3 - Absolute Strains, Test #4 - #5

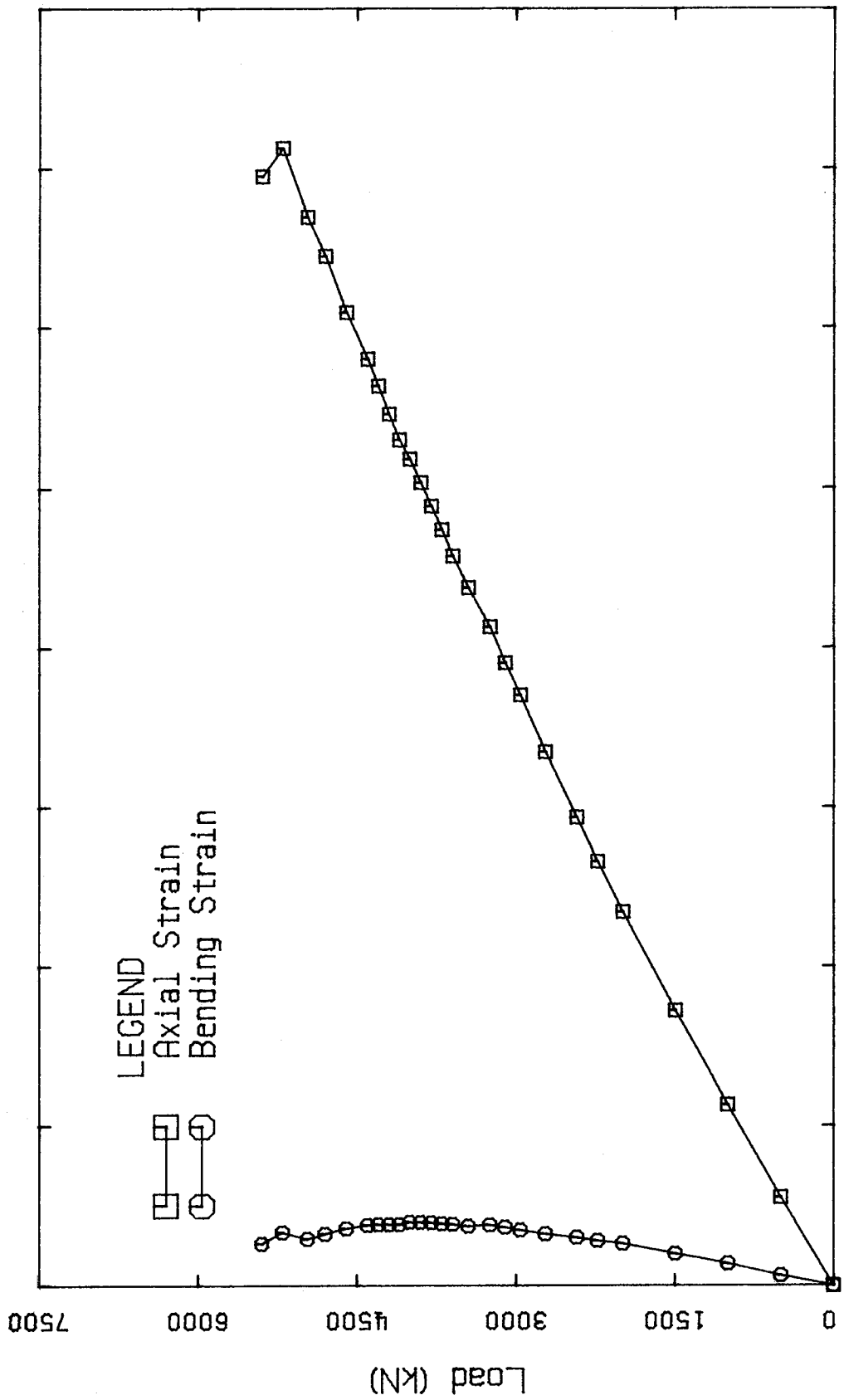

Figure 4.19 Section 4 - Absolute Strains, Test #4 - #5

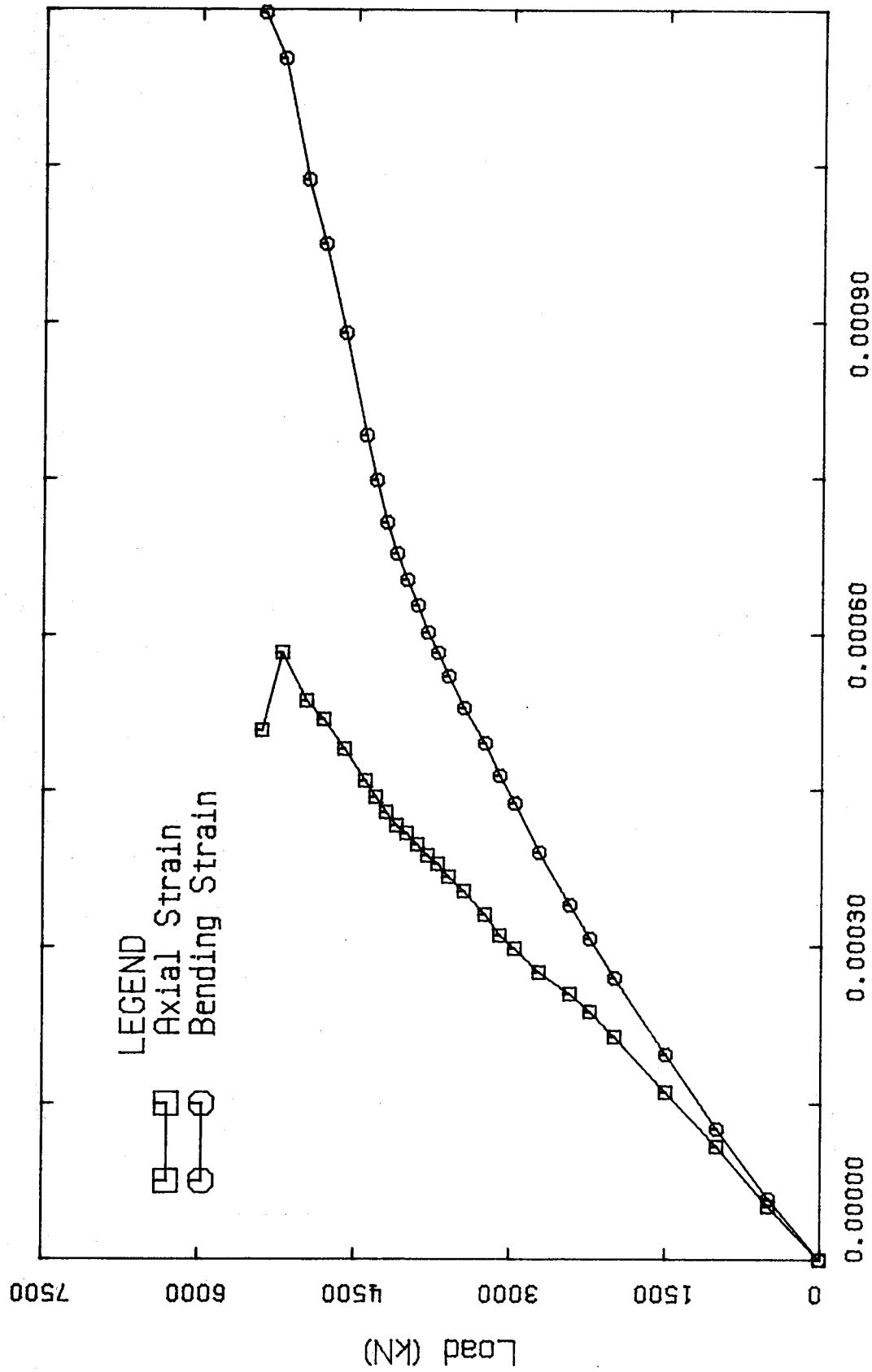

Figure 4.20 Section 5 - Absolute Strains, Test #4 - #5

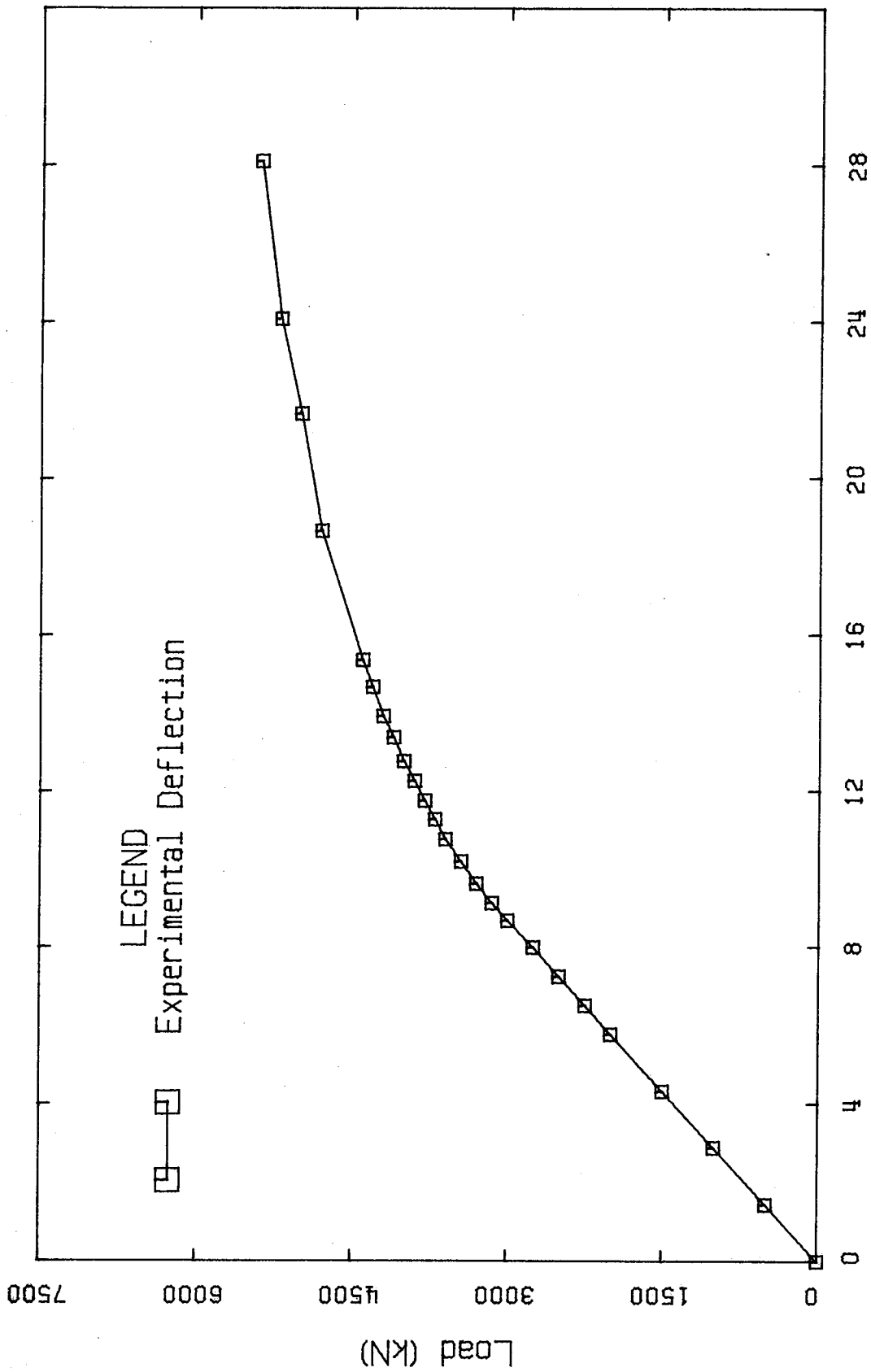

Figure 4.21 Load vs Deflection, Test #4 - #5

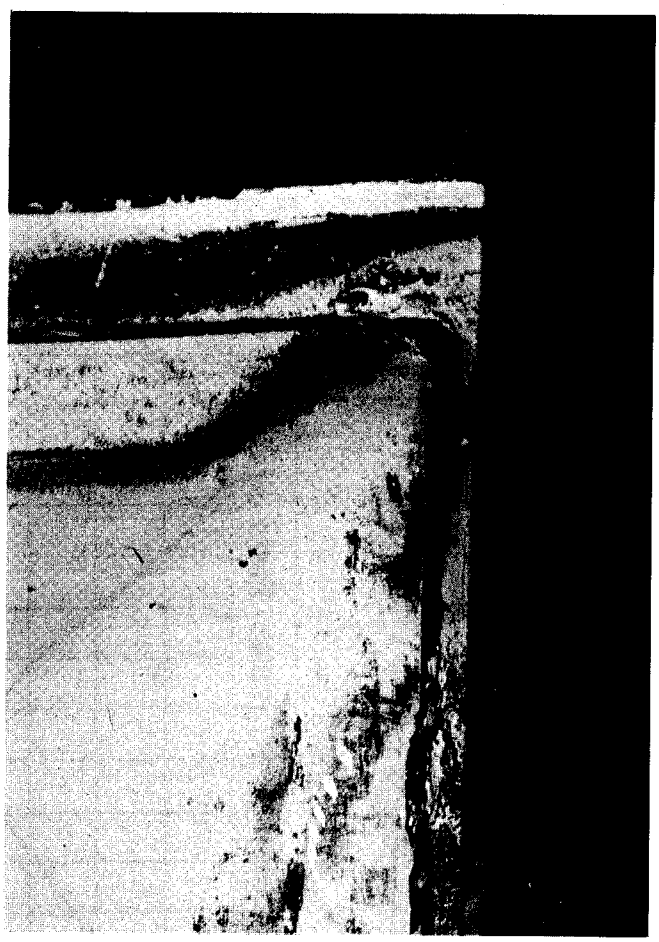

Figure 4.22 Weld Tear of Fish Plate Connection at 5200 kN

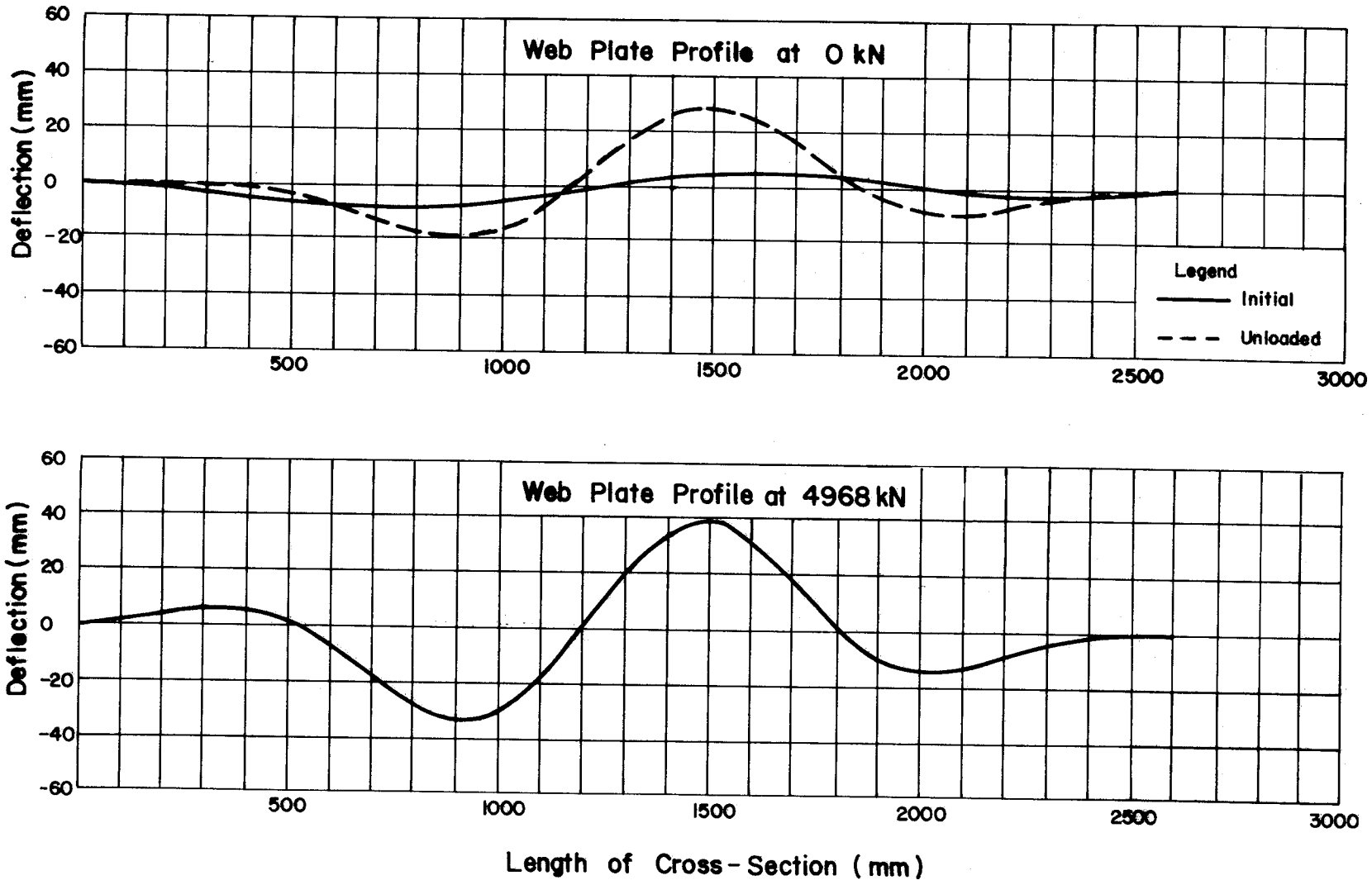

Figure 4.23 Web Deflection, Test #4

5. Comparison of Analytical and Experimental Results

5.1 Introduction

In this chapter, a comparison is made between the actual behavior of the frame and its predicted behavior. Framing member strains, web plate stresses, and overall frame deflections are examined.

5.2 Web Plate Stresses at Predicted First Yield

In Figure 5.1, the predicted versus experimental web plate stresses are shown for the load corresponding to first yield for the centerline gauges of Panel #1. Using the results of the coupon tests, a value of yield load (3352 kN) was calculated and the corresponding web stresses were derived from this value. At a load very close to the calculated yield, 3450 kN, strain readings were taken and the principal stresses were obtained. Figure 5.1 shows the comparison between the experimental and predicted results. Apart from the poor experimental results obtained at the second and fourth gauges from the top (both principal stresses are positive here), the general distribution agrees fairly well with that predicted by the model. The major difference between the two is that some of the experimental principal stresses tend to be inclined at a slightly steeper angle than do the calculated stresses. However, the central region of the plate shows that actual yielding (271 MPa) is occurring within the vicinity of this load. It is worth noting

that the calculated critical web buckling stress for a web plate having the dimensions of the test specimen is only 12 MPa.

In the lower two-thirds of the plate, the angle of inclination of the tension field, α, as obtained from the strain gauge readings varied between 46.6° and 53.2°. The predicted value of α was 51.0°.

5.3 Strains to Failure in Framing Members

A comparison between the calculated and actual strains in selected framing members is shown in Figures 5.2 through 5.4. To generalize, acceptable results are obtained when the sources of error involved with strain gauge response are understood. These are covered separately in Section 5.6.1. Measured strains at cross-sections 1 and 2 are at most variance with the predicted strains. The results from the remaining three gauged locations indicate good agreement between the modelled behavior of the frame and the measured values.

Figure 5.2 shows that there is good agreement between measured axial strains and the calculated axial strains for cross-section 2. It also shows that the measured bending strains for a given load are much lower than those predicted by the plane frame analysis. The magnitude of bending strains ultimately exceeds that of the axial, but only at the highest loads.

Good correlation between predicted and measured strains for both axial and bending effects at cross-section 4 is indicated in Figure 5.5. The measured axial strains are slightly larger than the calculated strains. Very little bending was present in the member, indicating consistency with the expected zero bending state.

Good agreement between experimental and predicted strains is present at cross-section 5 as well (see Figure 5.4). There is excellent agreement for axial strains throughout the loading. The measured bending strains are slightly less than predicted, but correlation improved as the test proceeded. In the case of cross-section 2, the twin cross-section, it is only the bending strains that vary significantly during the test (Figure 5.2).

In general, it appears that the calculated axial response agrees well with the measured values, whereas the actual bending behavior is less than that predicted. This implies that the moments are less than those predicted. The geometrical dissimilarities between the actual test frame and the analytical model may be partly the reason. This effect is examined in Section 5.6.2.

5.4 Frame Deflection to Failure

The load versus deflection curves for both the test and predicted response of the framing scheme are shown in Figure 5.5. There is remarkably good agreement between the two. The linear load limit of the test frame is approximately 3400

kN. When compared to the predicted linear load limit value of 3352 kN, an underestimate of only 1.4% is indicated. The error is 10.0% when comparing the predicted deflection of 9.00 mm to the 10.00 mm observed.

In the analysis, an incremental loading was used to develop the inelastic portion of the predicted curve. As each increment of load was applied, the frame was examined to see whether either portions of the web (the inclined bars) had yielded or whether the cross-section of a boundary member showed yielding. The analysis was done using a plane frame program founded on the stiffness approach. It used the framing idealization of the web plate as suggested by Thorburn, et al. (1) (see Figure 2.1). After yield (271 MPa) had been reached in a web tension member, that bar was modelled as being unable to carry any additional load. When a boundary member started to yield (under combined axial and bending loads), an effective softening was introduced into the frame. The critical cross-section of the element was modified by trial until it was in equilibrium with the applied forces.

The portion of the curve just beyond the yield load (linear load limit) shows that, at a given load, the experimental deflection is marginally greater than the corresponding calculated value. This occurs up to a load level of about 4725 kN. Following this, predicted deflections are greater than experimental values.

The post-elastic model used contains a number of simplifications that should be noted. Strain-hardening characteristics for both the web plate and framing members were not incorporated into the analytical technique. This no doubt results in an overestimate of the frame deflection in the inelastic range. Residual stresses, which would be present in the fabricated framing members, were neglected, and any yield affecting a cross-section was assumed to spread uniformly and parallel to the strong axis in bending. In addition, as has already been noted, the yielding was associated with the entire element, not just with the cross-section. Although the actual yield strength of the web material was used in the analysis, the minimum specified yield strength (300 MPa) had to be assumed for the boundary members.

It should also be recognized that the angle of inclination of the tension field was derived on the basis that the web plate behavior remains within the elastic range and that the stress field within the plate is uniform. The stress field is known to be non-uniform (1), and by definition portions of the web plate become inelastic after the linear load is exceeded. Finally, the effects of axial shortening of the columns have been neglected.

Figure 5.6 shows predicted load versus deflection curves for otherwise identical frames to that discussed here except that thinner web plates are substituted. What was desired was to examine hypothetical cases in which more, or

possibly all, of the tension diagonals of the web would yield prior to yield occurring in the framing members. For the case of a 3 mm thick web, only two tension members of ten yield prior to the first yield of surrounding boundary elements. For the 2 mm thick web, four tension members yield while for the last example (1 mm thick web), eight of the ten struts yield before any boundary elements yield. Thus, in this example, there is no case in which the web is entirely yielded prior to the first yielding of the framing members. (The remaining portion of the curves are not completed to ultimate load as the procedure is extremely time consuming and the required information has already been obtained.)

From the examination of the case where a 1 mm web plate is used, it is seen that successive deterioration of the tension diagonals leads to rapid decay of the structure's stiffness. It is also noted that a modest increase in the web plate thickness, can produce a substantial increase in framing stiffness. For practical applications, wherein web plates no thinner than 4 mm would be used, successive and widespread yielding will not occur throughout the plate at high loads for the geometry examined and framing members used herein.

5.5 Factors Affecting Failure

The sequence of events that led to the failure of the specimen was summarized in Section 4.4.4. As noted there, the ultimate load attained in the test was not governed by the frame itself, but resulted from a local failure. From examination of the actual load versus deflection history of the test specimen in Figure 4.21, it is seen that the slope of the curve during the final load increment is fairly flat. This would indicate that the maximum load achieved, 5395 kN, was probably close to the ultimate load that the frame might have attained.

It was noted earlier that the detail used to provide load transfer between the web plate and the framing members introduced an eccentricity. A misalignment of the fish plate (probably induced by the welding stresses) and a slight bend in both of the doubler plates of the pin-connection at the location of failure were also noticed prior to testing. The latter probably occurred during transportation of the specimen.

Because of the eccentricity, moments were present in the web plate connection and the welds were stressed transversely, that is, out-of-plane with respect to the connection alignment. Failure occurred as a result of a weld tear in the direction of the eccentricity. Further loading accentuated both the weld tear and tendancy for out-of-plane movement of the doubler plates.

5.6 Sources of Errors

Although great care was taken during all stages of preparation, set-up and testing, it is inevitable that the results are affected by errors in various parts of the loading and instrumentation systems and as a result of geometrical differences between actual and idealized values.

5.6.1 Instrumentation Errors

Strain gauges respond linearly only within a set voltage range. Balancing of the gauges (zeroing) prior to testing, in order that the gauge may respond equally well whether in tension or compression, was carried out for all strain gauges. Some difficulty was experienced in this operation where for some gauges the potentiometer on the signal conditioners reached its limit prior to initializing. The full elastic response range was therefore unavailable for these gauges.

Proper placement of the strain gauge onto the specimen is of prime importance. It is essential that linear strain gauges be placed parallel to the expected in-plane strain response. Bonding gauges to the specimen in a skew manner will give smaller strain results. Poor bonding between the gauge and the material to be tested will result in drift of strain readings. These effects are present to some extent in all experimental tests.

Additional resistance between the actual strain gauge resistor and the signal conditioner to which it is connected

may be acquired through the electrical resistance of the circuit lead wires. A three wire lead system for each gauge alleviates this problem. This is especially important where long leads are used. It is suggested that a three rather than two wire system be used when the leads exceed 30 meters. Since the lead lengths for this test were no greater than approximately 10 meters, their associated resistance contribution was probably insignificant.

There is 1% variation in the strain gauge factor used in transforming the change in voltage of the gauge to actual strain response. Deviation from a constant voltage supply from the power source to the strain circuit will obviously also induce unreliable readings.

5.6.2 Geometrical Differences

To account for the observed general trend of actual moments smaller than the predicted moments at all cross-sections examined, the dissimilarities between the test frame and the analytical model were examined. Greater stiffnesses than modelled exist in the pin-connection regions because of the web bearing plates provided. The stiffeners between the central beam and adjoining columns do not identically represent the continuation of column flanges. The plate thicknesses of the fish plate and the webs of the framing members are greater than the web panel itself. In the model, the web panel thickness is assumed to be effective to the centerlines of the framing members in the shear panel. Since the

actual plate thicknesses enclosed by these same dimensions in the specimen are greater at the boundaries (because of the fish plate and framing member webs), a stiffer exterior edge exists within the web plate than modelled. Furthermore, the actual fish plate connections at the pinned connection regions may not effectively anchor the tension field within the plate to the exterior frame. Although their influences are probably small, these factors may account for some minor redistribution of loads.

The above, however, do not offer justification for the bending strain discrepancies between cross-sections 2 and 5. What may have occurred was a small unbalance in load distribution between the east and west test panels. A minor amount of bending would therefore be expected to exist in the central framing member, as was in fact observed. Larger moments would be exhibited by one exterior beam than the other, also apparent from the test results. A check of the geometric properties of the two built-up beams revealed that the actual dimensions of section 5 were extremely close to the idealized dimensions. The linear dimensions at cross-section 2 were 1% to 2% smaller than specified. Although these differences are very minor they may account for a small amount of load unbalance. Furthermore, if simultaneous seating of the reaction points during the final compression test did not occur, some additional load unbalance would result.

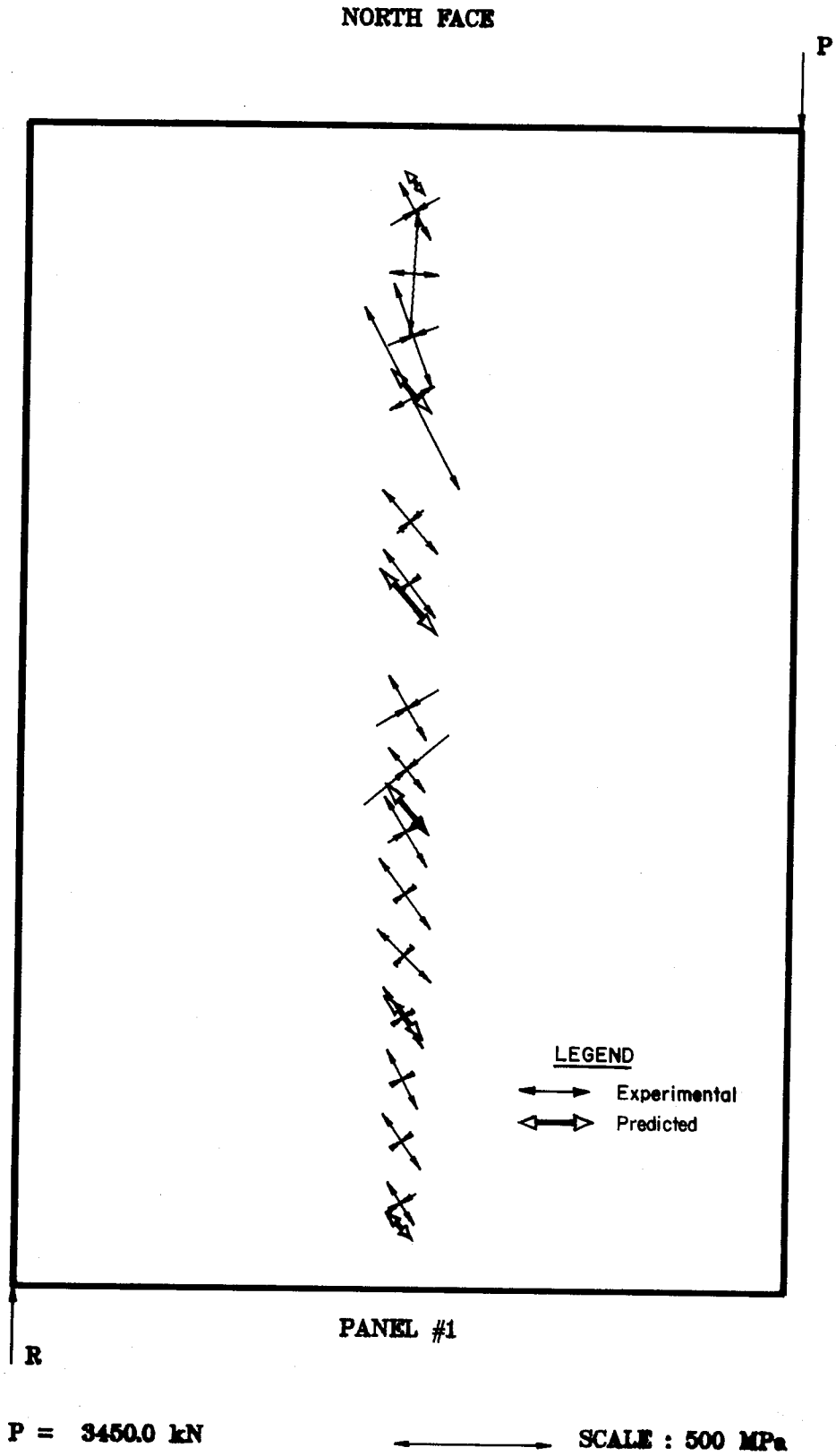

Figure 5.1 Predicted vs Experimental Web Stresses at Yield

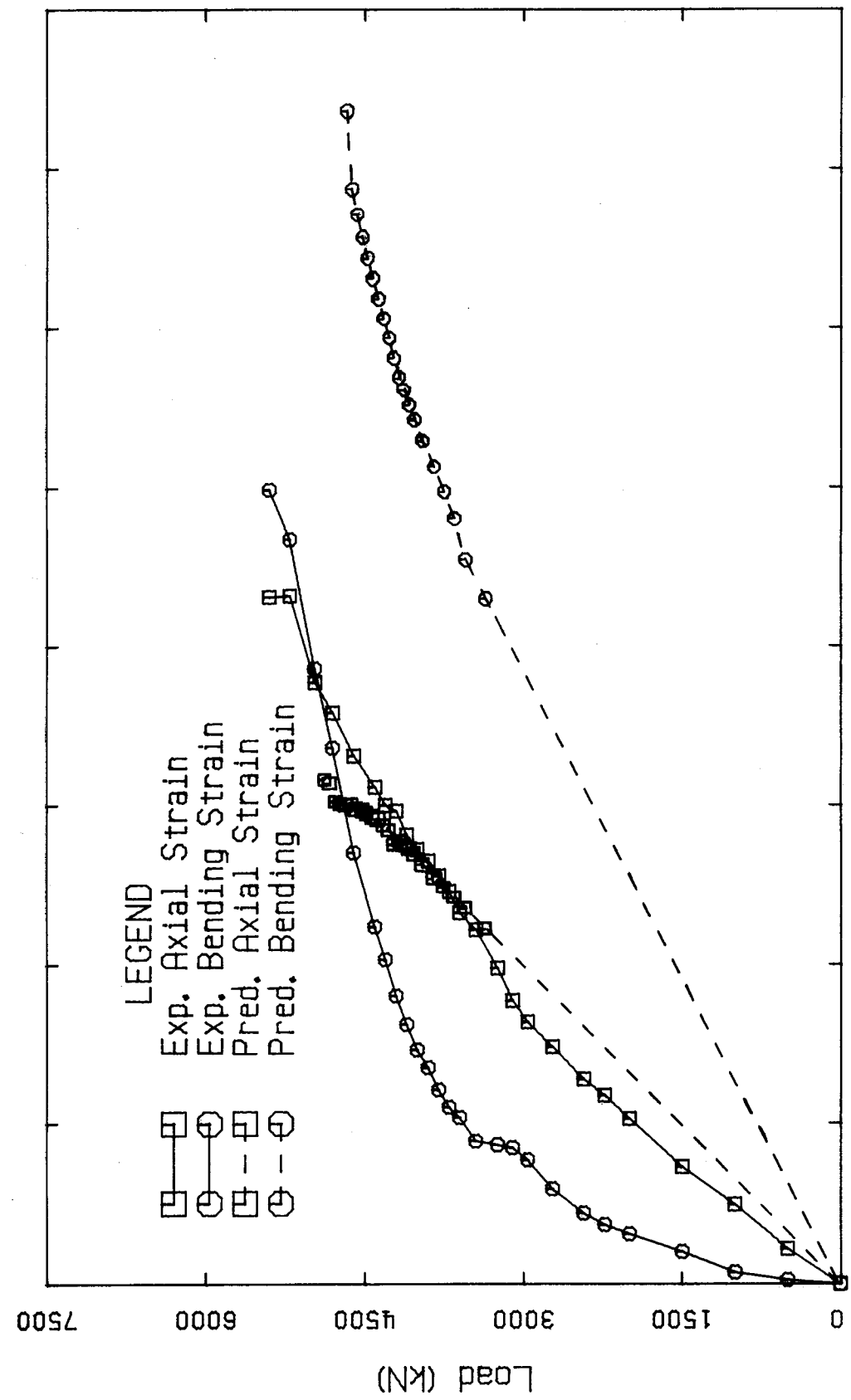

Figure 5.2 Section 2 - Predicted vs Experimental Strains

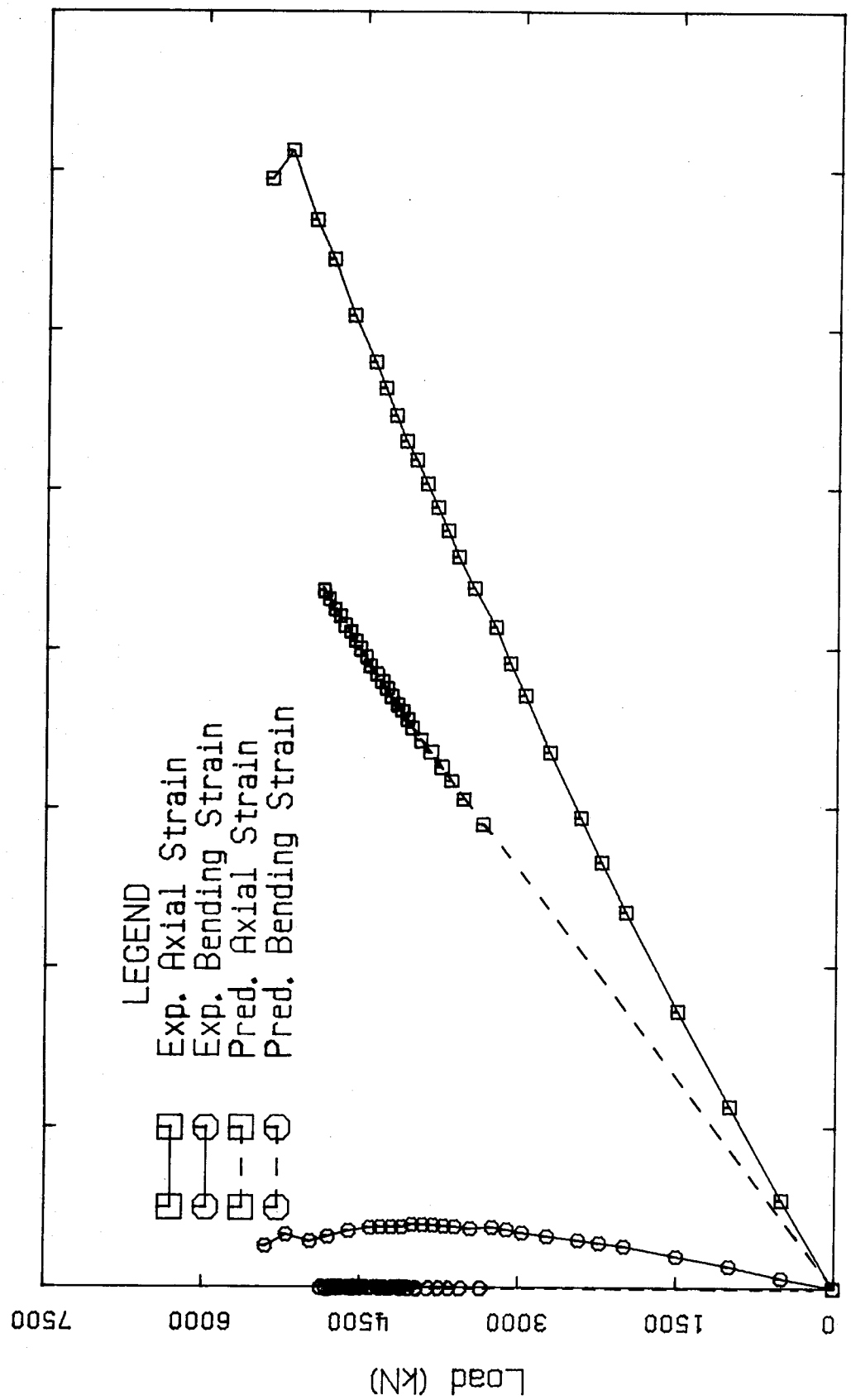

Figure 5.3 Section 4 - Predicted vs Experimental Strains

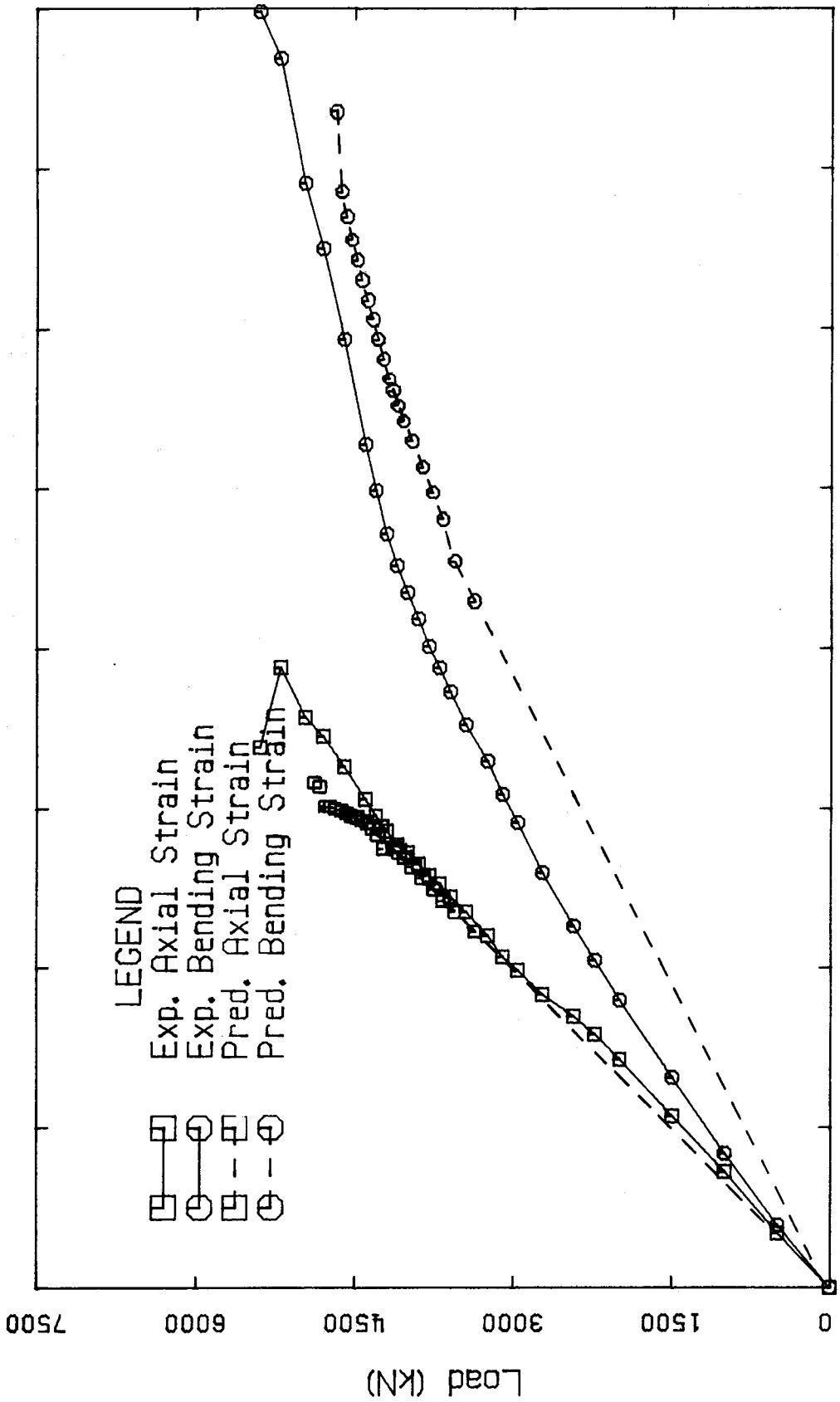

Figure 5.4 Section 5 - Predicted vs Experimental Strains

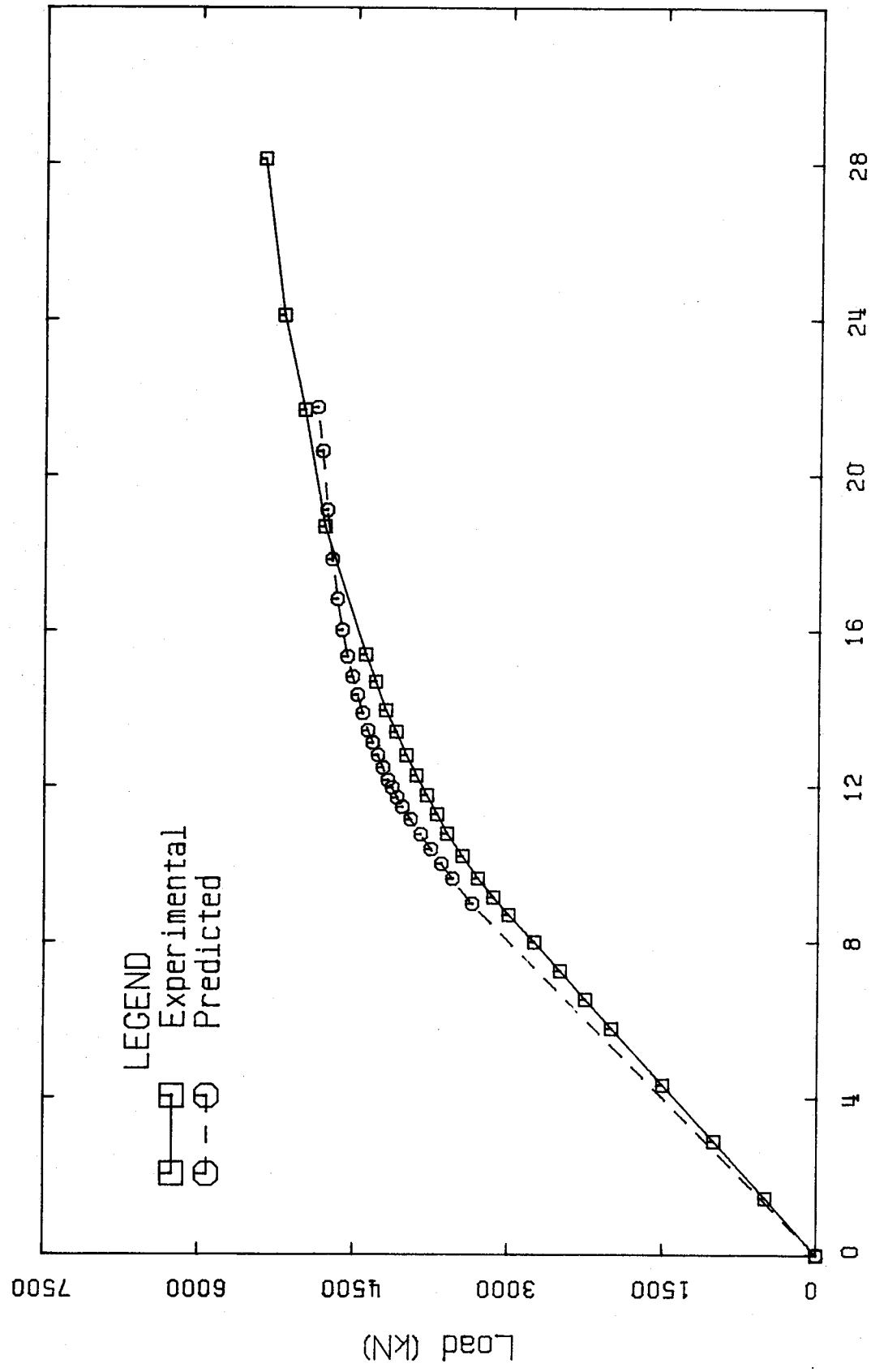

Figure 5.5 Predicted vs Experimental Frame Deflection

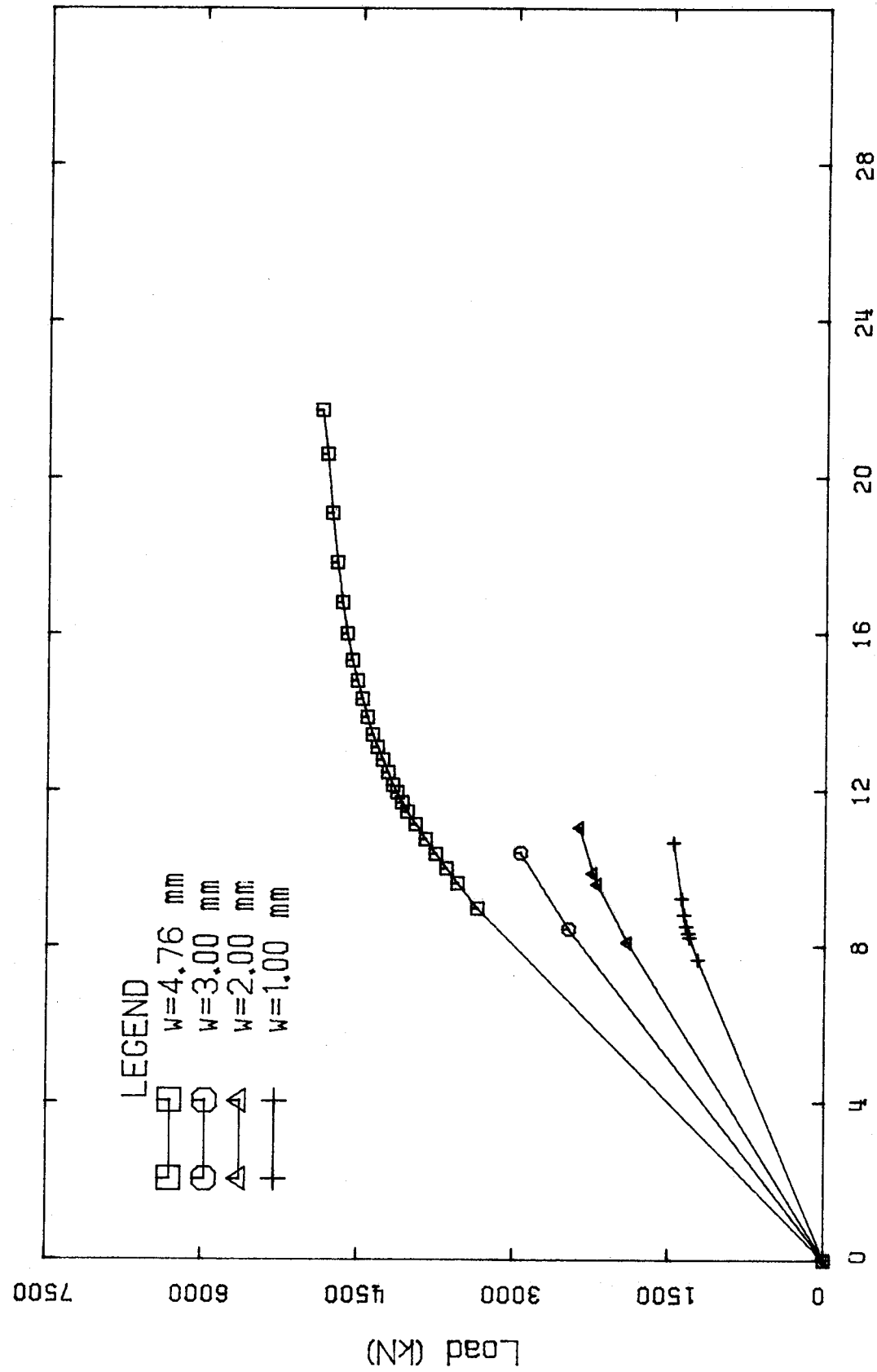

Figure 5.6 Predicted Frame Deflection Curves

6. Summary, Conclusions and Recommendations

6.1 Summary and Conclusions

The study reported herein describes the large-scale test of a steel plate shear wall subassemblage. The test specimen consisted of realistically sized components and was fabricated using standard shop practices. The analytical method developed by Thorburn, et al. (1), was used both to design the test specimen and to provide the basis for the test evaluation. Some shortcomings of the analytical method of Thorburn were noted and modifications have been suggested (Appendix A). The test also allowed for observations to be made about the fabrication details used.

Loading of the specimen was done in an incremental fashion to two distinct levels; service and ultimate. A cyclical load application to the permissible deflection limit in each direction was performed three times. Following this, a final test to the ultimate capacity of the test frame was conducted. The test specimen was subjected to lateral loads much greater than those expected in the lower levels of a typical shear core. Although column loads were not explicitly applied in the test set-up, induced axial compressive stresses were of course, present. Measured compressive loads in the columns at the service load level were approximately 11% of the column yield load. Column axial loads in prototype structures are generally in the order of 30% to 50% of the yield load.

The following descriptions summarize the findings of the steel shear wall test.

Good correlation between predicted and actual web plate stresses was apparent. The angle of inclination of the principal stresses was in the order of -9% to +4% of that predicted, whereas the averaged measured orientation of buckle and yield band formation were between 3% and 14% less.

The measured axial framing member strains showed good to excellent correlation as compared to the predicted values. Poorer correlation was obtained between measured bending strains and calculated bending strains; in each case, the measured strains were lower than those predicted.

Accurate prediction of the entire load versus deflection response was obtained using a quasi-elastic approach. Based on load, modelling of the location of the end of the linear range was underestimated by only 1.4%. The frame showed good ductility when loaded to its ultimate capacity.

The discrepancies found in the original derivation of the angle of inclination (1) were of minor significance. The revised formula, presented in Appendix A, should be used for a more accurate description of the angle of the tension field.

From the results obtained and analysed during the test life of the single full scale specimen, it is concluded that the simplified analytical method for thin-webbed steel shear walls, as offered by Thorburn, et al., is a satisfactory approach.

6.2 Recommendations

6.2.1 Fabrication Techniques

Several suggestions as to fabrication techniques are made with particular reference to multi-storey steel shear wall tiers following the observations made during this single study.

Special attention must be paid to the corner connection details to ensure that a continuous stiff boundary is provided for the proper anchoring of the tension field within the plate. Unnecessary out-of-flatness of the plate can be avoided by supporting the plate in the center, thereby minimizing its sag, if shop welding is done in the horizontal position. Although the one-sided fish plate connection results in an eccentricity of load, problems as a result of this occurred only at extremely high loads. Satisfactory performance was displayed at service load levels. Fabricators can best judge whether the substitution of a two-plate connection with intermittent welds is economically justified.

With regard to fireproofing of the web plate, the test showed that the buckles formed were not steep in profile and therefore should not present any undue difficulty in either attaching or maintaining the integrity of fireproofing materials throughout at least the serviceability range.

6.2.2 Future Testing

Although the test reported is not considered to present any serious shortcomings, more tests are always desirable. The multi-storey response of this framing method should be examined in order to verify additional basic assumptions made in the analysis. A three storey segment wherein realistic gravity loads, applied to the columns, and transverse shears applied at floor levels, is suggested for testing at both a cyclic service load level and to ultimate.

References

1. Thorburn,L.J., Kulak,G.L., and Montgomery,C.J., *Analysis and Design of Steel Shear Wall Systems*, Structural Engineering Report No. 107, Department of Civil Engineering, University of Alberta, Edmonton, Alberta, May 1983.

2. Basler,K., *Strength of Plate Girders in Shear*, Journal of the Structural Division, ASCE, Vol. 87, No. ST7, Proc. Paper 2967, Oct. 1961.

3. Wagner,H., *Flat Sheet Metal Girders with Very Thin Metal Webs. Part I--General Theories and Assumptions*, National Advisory Commitee for Aeronautics, Technical Memo., No. 604, 1931.

4. Kuhn,P., Peterson,J.P., and Levin,L.R., *A Summary of Diagonal Tension, Part I--Methods of Analysis*, National Advisory Commitee for Aeronautics, Technical Note 2662, 1952.

5. Johnston,B.G., Editor, The Structural Stability Research Council Guide to Stability Design Criteria for Metal Structures, Third Edition, John Wiley & Sons, Inc., New York, N.Y., 1976.

6. Dowling,P.J., Harding,J.E., and Frieze,P.A., Steel Plated Structures, An International Symposium, Crosby Lockwood Staples, Publishers, London, England, 1977.

7. *Shear Walls and Slip-Forming Speed Dallas' Reunion Project*, Engineering News-Record, July 28, 1977.

8. *Quake-Proof Hospital has Battle-Ship Like Walls*, Engineering News-Record, Sept. 21, 1978.

9. *Steel Shear Walls for Existing Buildings*, Engineering Journal, AISC, Vol. 20, No. 2, Second Quarter, 1983.

10. Angelidis,N., and Mansell,D.S., *Steel Plate Cores in Tall Buildings*, Transactions of the Institution of Engineers, Australia, Civil Engineering, Vol. CE24.No. 1, February 1982.

11. Angelidis,N., and Mansell,D.S., *Fabrication of Steel Service Cores for Multi-Storey Buildings*, Transactions of the Institution of Engineers, Australia, Civil Engineering, Vol. CE24.No. 1, February 1982.

12. Coull,A., and Choudhury,J.R., *Analysis of Coupled Shear Walls*, J. Am. Conc. Inst., Vol. 64, September 1967.

13. Michael,D., *Effect of Local Wall Deformations on the Elastic Interaction of Cross Walls Coupled by Beams*, Proc. Symp. on Tall Buildings, Southampton University, England, 1966.

14. Timoshenko,S.P., Elements of Strength of Materials, Fifth Edition, Van Nostrand Reinhold, Publishers, Princeton, N.J., 1968.

15. Takahashi,Y., Takeda,T., Takemoto,Y., and Takagi,M., *Experimental Study on Thin Steel Shear Walls and Particular Steel Bracings Under Alternative Horizontal Load*, Preliminary Report, IABSE Symposium on Resistance and Ultimate Deformability of Structures Acted on by Well-Defined Repeated Loads, Lisbon, Portugal, 1973.

16. CSA CAN3-S16.1-M78, Steel Structures for Buildings--Limit States Design, Canadian Standards Association, Rexdale, Ontario, 1978.

17. Troy,R.G., and Richard,R.M., *Steel Plate Shear Walls Resist Lateral Loads, Cut Costs*, Civil Engineering, ASCE, Vol. 49, Feb. 1979.

18. *Nippon Steel Building at Urban Renewal at Tokiwabashi District*, Private Correspondance with CISC, Jan. 1980.

19. Chien,E., *Steel Plate Shear Wall Structures in Tokyo, Japan*, Private Correspondance with CISC, Jan. 1980.

20. *A Guide to the Structure of B-Class Japanese Buildings*, Private Correspondance with CISC, Jan. 1980.

21. *Structural Design of Shinjuku Nomura Tower*, Notes from a meeting of ASCE-IABSE Joint Committee for Planning and Design of Tall Buildings, Tokyo, Japan, Sept. 1976, Private Correspondance with CISC, Jan. 1980.

22. *Patent Problems, Challenge Spawn Steel Seismic Walls*, Engineering News-Record, Jan. 26, 1978.

23. *Hospital Steel Plate Shear Walls were Designed for a 0.69G Earthquake*, Architectural Record, August 1978.

24. *Steel Plate Shear Walls Blunt the Wind's Force and Carry Gravity Load in a Towered Hotel*, Architectural Record, August 1978.

25. *Shear Walls and Slip-Forming Speed Dallas' Reunion Project*, Engineering News-Record, July 28, 1977.

26. Bleich,F., Buckling Strength of Metal Structures, McGraw-Hill Book Company, Inc., New York, N.Y., 1952.

27. Wang,T.K., *Bucking of Transversly Stiffened Plates Under Shear*, Journal of Applied Mechanics, Vol. 14, 1947.

28. Bathe,K.J., Wilson,E.L., and Peterson,F., SAP#IV, A Structural Analysis Program for Static and Dynamic Response of Linear Systems, Earthquake Engineering Research Centre, Report No. EERC 73-11, College of Engineering, University of California, 1974.

29. *California Hospital is Quake-Proof, High-Rise*, Engineering News-Record, August 10, 1978.

30. *Hospital Design Meets Tough Seismic Code*, Engineering News-Record, April 21, 1977.

31. *Hospital's Bracing is Eclectic Mix*, Engineering News-Record, Dec. 24, 1981.

32. Popov,E.P., Mechanics of Materials, Prentice-Hall, Inc., Englewood Cliffs, N.J., 1978.

33. Salmon,C.G., and Johnson,J.E., Steel Structures: Design and Behavior, Second Edition, Harper and Rowe, Publishers, New York, N.Y., 1980. Chapter 6, Part II.

34. American Institute of Steel Construction, Specification for the Design, Fabrication, and Erection of Steel Structures for Buildings, New York, N.Y., 1978.

35. Timoshenko,S.P., and Goodier,J.N., Theory of Elasticity, Third Edition, McGraw-Hill Book Co. Inc., New York, N.Y., 1970.

Appendix A

Formula Derivation for
Angle of Inclination of Tension Field

A.1 Formula Derivation

A derivation for the angle of inclination of the tensile field within the web plate of a shear panel subjected to transverse loading was first presented by Wagner following his study on flat aluminum sheet metal girders (3). Relating the boundary conditions surrounding the web panel studied by Wagner to those of a shear core panel within a structure, Thorburn, et al. (1), concluded that the formulation for this case did not differ from that derived by Wagner. Specifically, the work expression involved considered the energy absorbed only by the axial forces within the system as a result of an assumed uniform tension field within the plate. Several additional postulations were made in the modelling to simplify the formulation. The web energy associated with the compressive forces perpendicular to the tension field was expected to be negligible since the plate offers little resistance to buckling. Furthermore, the low energy absorbtion as a result of shear within the framing members was also omitted.

Upon further examination of the derivation for the angle of inclination of the tension field during the study reported herein, it was considered that the contribution of an additional effect should be included. Since the columns have an unbalanced force acting on one flange face as a result of the tension field, they are subject to bending. The associated bending strain energy term for the columns should therefore be included in the energy summation. It was

considered necessary to re-evaluate the derivation of the angle of diagonal tension field recognizing this additional effect. For completeness the entire derivation, including the column bending term, is presented in this appendix.

Consider first the free-body diagram of Figure A.1, showing a typical shear core subjected to lateral loads. The total shear V is assumed to be resisted by the web plate alone. Since the web is idealized as being connected to the centerlines of the framing members, only half of each column web is neglected for shear transfer. This will not be significant. (It is customary to neglect the flanges of I sections when calculating the shear resistance of a member.)

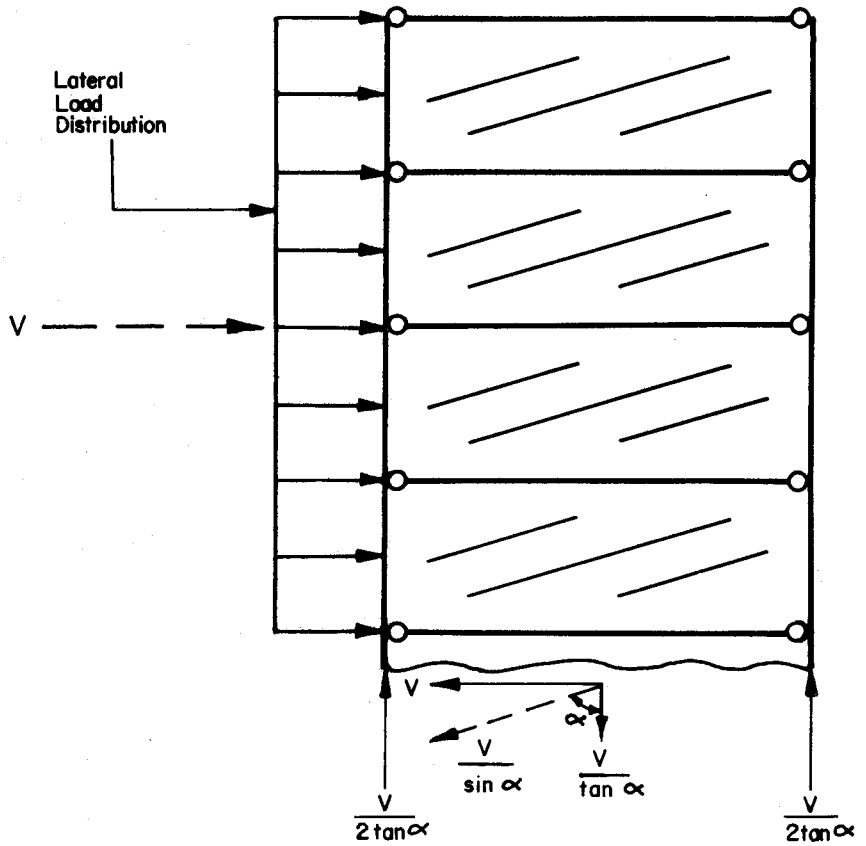

Figure A.1 Shear Core Subjected to Lateral Load

Recognizing that the horizontal resistance V is only a component of the tension field within the plate, the other components of the force triangle can be calculated, as shown in the figure. The notation α is used for the angle of inclination of the tension field. It is further assumed that the tension field within the web will be constant. (The actual distribution of the stress field is dependent upon the stiffness of the boundary members.) Thus, the vertical component of the tension field force is divided equally to the two columns.

Because the ratio of adjacent floor level shears approaches unity rather quickly for usual load cases, the tension fields bounding an interior beam are assumed to be equal (see Figure A.2). Therefore, vertical load transfer as a result of the shear within the web panel is effected through the columns only.

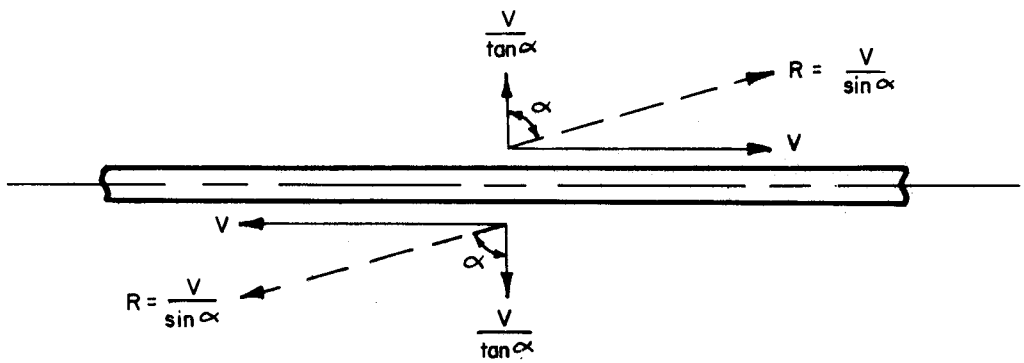

Figure A.2 Balancing Tension Fields

The web plate is examined next. Shown in Figure A.3 is a portion of web with depth equal to the column height, h.

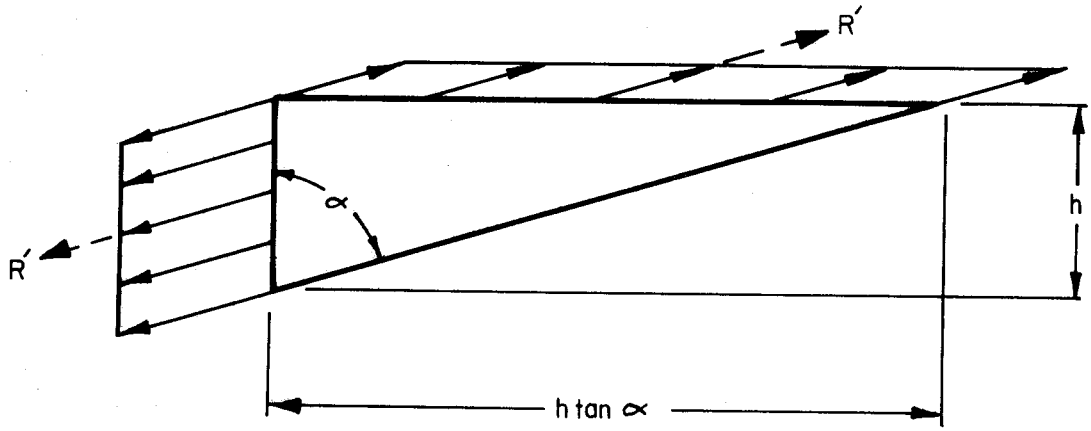

Figure A.3 Free-Body Diagram of Portion of the Web

Note that no forces are shown along the diagonal cut. Since this cut is coincident with the direction of principal stress, shear stresses are zero. The work contributed by the compressive stress is assumed to be negligible compared to the other terms. Therefore, no compressive force is shown along the cut.

The inclined force on the beam (Figure A.2) can be expressed in terms of force per unit length, $V/L\sin\alpha$. Thus, the total force along the horizontal portion of the web identified in Figure A.3 is;

$$R' = \frac{V}{L \sin\alpha} (h \tan\alpha) = \frac{Vh}{L \cos\alpha}$$

Because the vertical portion of the web shown in Figure A.3 must be anchored by the column, force R' also acts on the column. Its horizontal component is $R'\sin\alpha = V h \tan\alpha / L$, and its vertical component is $R'\cos\alpha = Vh/L$.

A free-body diagram of the left hand column is shown in Figure A.4. It extends from the midstorey of one panel to the midstorey of another. (Moments exist at the column mid-heights; they are not shown in the figure.)

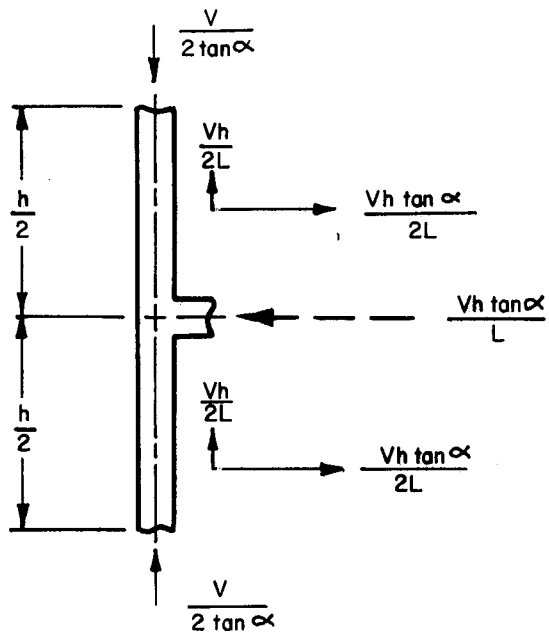

Figure A.4 Column Free-Body Diagram

Summation of forces in the horizontal direction gives the beam axial force. A further simplification is introduced here since the applied lateral load which should show up at the floor level is not included in the summation. Thus, the resultant axial force in the beam is taken as constant at a value $V h \tan\alpha / L$ when in fact it has a linearly varying shape.

In a similar way, the column axial force will be taken in a simplified way as a value $V/2\tan\alpha$ (see Figure A.4). Its true shape is also one which varies linearly as the vertical components of the tension field force are applied along the length of the column.

Finally, the bending effect of the horizontal component of the tension field force acting on the column will be identified. Considering the column to act as a continuous member over a series of supports spaced at h, the moment diagram is that for a fixed ended beam. Thus, for an applied horizontal load per unit length of $V\tan\alpha/L$, the end moments are $Vh^2\tan\alpha/12L$ and the mid-height moment (of opposite sign) is $Vh^2\tan\alpha/24L$.

On the basis of the force distributions within the frame resulting from only the tension field forces, the energy equation can now be formulated. For a typical panel, the energy within the frame consists of contributions from the web, one beam, and two columns. The work components of each will be evaluated separately and then summed to give the total internal work performed by the panel when subjected to a tension field. Thus,

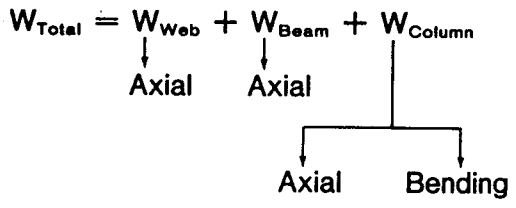

and a column length h. Recalling that two columns are involved, the resulting expression for this contribution to the work is:

$$W_{c_{Axial}} = \frac{V^2 h}{4A_c E \tan^2\alpha} \qquad (A.3)$$

Finally, for the portion of the column strain energy due to bending, the general expression is;

$$W = \int_L \frac{M^2}{2EI}\, dx$$

The moment distribution in the column is parabolic and can be expressed as:

$$M_c = \frac{z}{12}(6hx - h^2 - 6x^2)$$

where z = Vtanα/L, the uniformly distributed load along the column flange face resulting from the tension field. Substitution and integration over both columns gives;

$$W_{c_{Bend}} = \frac{V^2 h^5 \tan^2\alpha}{720\, E\, I_c L^2} \qquad (A.4)$$

The total work expression then, is the summation of Equations A.1 through A.4.

$$W_{Total} = \frac{V^2 h}{2\, Ew\, L \cos^2\alpha \sin^2\alpha} + \frac{V^2 h^2 \tan^2\alpha}{2A_b\, E\, L} + \frac{V^2 h}{4A_c E \tan^2\alpha} + \frac{V^2 h^5 \tan^2\alpha}{720\, E\, I_c\, L^2} \qquad (A.5)$$

Simplification of Eq. A.5 results in:

$$W_{Total} = \frac{V^2 h}{2E}\left(\frac{1}{wL \cos^2\alpha \sin^2\alpha} + \frac{h \tan^2\alpha}{A_b L} + \frac{1}{2A_c \tan^2\alpha} + \frac{h^4 \tan^2\alpha}{360\, I_c\, L^2}\right)$$

Minimizing this relationship by taking the first derivative with respect to α and setting the resulting equation equal

to zero gives,

$$\tan^4\alpha = \frac{\frac{2}{wL} + \frac{1}{A_c}}{\frac{2}{wL} + \frac{2h}{A_b L} + \frac{h^4}{180\, I_c\, L^2}} \qquad (A.6)$$

or,

$$\alpha = \tan^{-1}\sqrt[4]{\frac{1 + \frac{wL}{2A_c}}{1 + wh\left(\frac{1}{A_b} + \frac{h^3}{360\, I_c\, L}\right)}} \qquad (A.7)$$

It is interesting to compare this to the former solution, originally postulated by Wagner (3) and followed by Thorburn, et al. (1), namely;

$$\alpha = \tan^{-1}\sqrt[4]{\frac{1 + \frac{wL}{2A_c}}{1 + \frac{wh}{A_b}}} \qquad (A.8)$$

Appendix B

Determination of Angle of Inclination of Tension Field for the Test Specimen

B.1 Theoretical Value of Tension Field Angle

The concepts developed in Appendix A were used to determine the angle of theoretical inclination of the tension field for the test specimen. Because the boundary conditions for the test specimen were different in some respects from those described in Figure A.1, some modifications were necessary. The assumptions were the same as the previous derivation for a panel subjected to shear except for two aspects. The true boundary conditions for the columns were fixed at one end and pinned at the other. Secondly, the "exterior" beam of the panel was free to bend, and the additional bending strain energy of one beam was therefore introduced to the total work equation. The other beam, the central one in the test specimen, would exhibit no bending because of symmetry of loading.

Following the same procedure of analysis for the model as done in Appendix A, but including the changes just noted, the solution for α is;

$$\alpha = \tan^{-1} \sqrt[4]{\frac{1 + wL\left(\frac{1}{2A_c} + \frac{L^3}{120\, I_b h}\right)}{1 + wh\left(\frac{1}{2A_b} + \frac{h^3}{320\, I_c L}\right)}} \qquad (B.1)$$

The last entry in the numerator is the additional contribution due to bending of the one beam member. The final term in the denominator reflects the change in the boundary conditions when compared to Eq. A.7.

The following specification values for the test specimen were used in Eq. B.1;

It would seem more reasonable to use measured values; however, there is no evidence any measurement of actual geometry was done.

w = 4.763 mm (3/16" plate thickness)

L = 3750 mm

h = 2500 mm

A_b = 20 952 mm^2

I_b = 810.3 x 10^6 mm^4

A_c = 15 656 mm^2

I_c = 295.4 x 10^6 mm^4

Using these values, the theoretical angle α for the test specimen was calculated as 51.0°.

it is 52.79°, using these values and Eq, B.1

Using CISC values for W410×144 & W310×129 (which the beam & column member are compared to), α = 53.24°

Beam member used (from shop drawings)(Not mentioned in paper)

t = 25 w = 16 A = 20952 mm^2

b = 284 d = 472 I = 810.26 × 10^6 mm^4

Column member used

t = 20 w = 12 A = 15656 mm^2

b = 308 d = 318 I = 295.41 × 10^6 mm^4

Using Eq. A.7 α = 43.15°

A.8 α = 45.01°

RECENT STRUCTURAL ENGINEERING REPORTS

Department of Civil Engineering

University of Alberta

83. *Inelastic Behavior of Multistory Steel Frames* by M. El Zanaty, D.W. Murray and R. Bjorhovde, April 1980.

84. *Finite Element Programs for Frame Analysis* by M. El Zanaty and D.W. Murray, April 1980.

85. *Test of a Prestressed Concrete Secondary Containment Structure* by J.G. MacGregor, S.H. Simmonds and S.H. Rizkalla, April 1980.

86. *An Inelastic Analysis of the Gentilly-2 Secondary Containment Structure* by D.W. Murray, C. Wong, S.H. Simmonds and J.G. MacGregor, April 1980.

87. *Nonlinear Analysis of Axisymmetric Reinforced Concrete Structures* by A.A. Elwi and D.W. Murray, May 1980.

88. *Behavior of Prestressed Concrete Containment Structures - A Summary of Findings* by J.G. MacGregor, D.W. Murray, S.H. Simmonds, April 1980.

89. *Deflection of Composite Beams at Service Load* by L. Samantaraya and J. Longworth, June 1980.

90. *Analysis and Design of Stub-Girders* by T.J.E. Zimmerman and R. Bjorhovde, August 1980.

91. *An Investigation of Reinforced Concrete Block Masonry Columns* by G.R. Sturgeon, J. Longworth and J. Warwaruk, September 1980.

92. *An Investigation of Concrete Masonry Wall and Concrete Slab Interaction* by R.M. Pacholok, J. Warwaruk and J. Longworth, October 1980.

93. *FEPARCS5 - A Finite Element Program for the Analysis of Axisymmetric Reinforced Concrete Structures - Users Manual* by A. Elwi and D.W. Murray, November 1980.

94. *Plastic Design of Reinforced Concrete Slabs* by D.M. Rogowsky and S.H. Simmonds, November 1980.

95. *Local Buckling of W Shapes Used as Columns, Beams, and Beam-Columns* by J.L. Dawe and G.L. Kulak, March 1981.

96. *Dynamic Response of Bridge Piers to Ice Forces* by E.W. Gordon and C.J. Montgomery, May 1981.

97. *Full-Scale Test of a Composite Truss* by R. Bjorhovde, June 1981.

98. *Design Methods for Steel Box-Girder Support Diaphragms* by R.J. Ramsay and R. Bjorhovde, July 1981.

99. *Behavior of Restrained Masonry Beams* by R. Lee, J. Longworth and J. Warwaruk, October 1981.

100. *Stiffened Plate Analysis by the Hybrid Stress Finite Element Method* by M.M. Hrabok and T.M. Hrudey, October 1981.

101. *Hybslab - A Finite Element Program for Stiffened Plate Analysis* by M.M. Hrabok and T.M. Hrudey, November 1981.

102. *Fatigue Strength of Trusses Made From Rectangular Hollow Sections* by R.B. Ogle and G.L. Kulak, November 1981.

103. *Local Buckling of Thin-Walled Tubular Steel Members* by M.J. Stephens, G.L. Kulak and C.J. Montgomery, February 1982.

104. *Test Methods for Evaluating Mechanical Properties of Waferboard: A Preliminary Study* by M. MacIntosh and J. Longworth, May 1982.

105. *Fatique Strength of Two Steel Details* by K.A. Baker and G.L. Kulak, October 1982.

106. *Designing Floor Systems for Dynamic Response* by C.M. Matthews, C.J. Montgomery and D.W. Murray, October 1982.

107. *Analysis of Steel Plate Shear Walls* by L. Jane Thorburn, G.L. Kulak, and C.J. Montgomery, May 1983.

108. *Analysis of Shells of Revolution* by N. Hernandez and S.H. Simmonds, August 1983.

109. *Tests of Reinforced Concrete Deep Beams* by D.M. Rogowsky, J.G. MacGregor and S.Y. Ong, September 1983.

110. *Shear Strength of Deep Reinforced Concrete Continuous Beams* by D.M. Rogowsky and J.G. MacGregor, September 1983.

111. *Drilled-In Inserts in Masonry Construction* by M.A. Hatzinikolas, R. Lee, J. Longworth and J. Warwaruk, October 1983.

112. *Ultimate Strength of Timber Beam Columns* by T.M. Olatunji and J. Longworth, November 1983.

113. *Lateral Coal Pressures in a Mass Flow Silo* by A.B.B. Smith and S.H. Simmonds, November 1983.

114. *Experimental Study of Steel Plate Shear Walls* by P.A. Timler and G.L. Kulak, November 1983.